

“Numerical Analysis of Natural Convection of Dual Nuclear Reactors embedded within a Square Enclosure through Porous medium and air”

Govindarao Nammi^{a,b}

a Department of Mechanical Engineering, National Institute of Technology Silchar, Silchar, 788010, India

b Department of Mechanical Engineering, GMR Institute of Technology, Rajam, 532127, India

Abstract

The present study portrays the role of distance when natural convection heat transport occurs by means of two embedded Micro-Nuclear-Reactors in a square enclosure with porous medium. The distances (distance $S=0.1, 0.2, 0.3, 0.4$) between the Micro-Nuclear-Reactors, along with Rayleigh and Darcy numbers ($10^3 \leq Ra \leq 10^6$) and ($10^{-4} \leq Da \leq 10^{-2}$), in numerical simulations by using COMSOL Multiphysics. As results, it is found that, before an optimal Ra value, the flow of heat remains symmetric but afterwards becomes asymmetric with increasing Ra to a greater extent changing the flow and temperature patterns in the enclosure. Results show that for every tenfold increase in Rayleigh number, the maximum streamline function, maximum temperature T_{max} , and minimum temperature T_{min} increases about tenfold, thus supporting the idea that buoyancy forces play a very important role in flow as well as heat transfer. Optimal heat transfer configuration was realized at reactor spacing of $s = 0.3$ when $Ra = 10^6$ and $Da = 10^{-2}$. Under these conditions, the Nusselt number had increased strongly due to the development of strong, independent convective cells around each reactor and the maximum possible heat transfer through convection. For shorter distances, $s = 0.1$, interaction between reactors was limiting the development of fully developed convective currents and therefore enhanced heat transfer efficiency. Greater separation distances, as in the case of $s = 0.4$, resulted in more isolated flow patterns. However, the overall benefits of heat transfer were lost since interaction between the reactors was reduced. But $Da = 10^{-2}$ shows the presence of stronger convective currents in the porous medium because of greater permeability, and this leads to a 27.7% improvement in the Nusselt number at the same distance and Rayleigh number above that for an air medium. For lower permeability conditions, $Da = 10^{-4}$, the motion of the fluid is restricted, and, thus, the transfer efficiency decreases significantly at higher Rayleigh numbers. These results are important in improving thermal management in applications such as nuclear energy production, electronics cooling, and the aerospace industry.

Keywords: Natural or free convection · Porous enclosure · Nuclear reactor, Interspacing distance ·

NOMENCLATURE

L	Enclosure length, m
g	Gravity of acceleration, ms^{-2}
h	Coefficient of heat transfer, $\text{Wm}^{-2}\text{K}^{-1}$
k	Thermal heatconductivity $\text{Wm}^{-1}\text{K}^{-1}$
Nu_t	Averaged or meanNu
p	Parameter for Pressure, Nm^{-2}
P	Non-dimensional pressure parameter
Pr	Prandtl number
Da	Darcy number
Gr	Grashof number
Ra	Ra
T_h	The temperature of bottom wall, K
T_c	The temperature of top wall of the enclosure, K
u,v	Components of velocity in x and y directions, ms^{-1}
U,V	Non-dimensional components of velocity in X and Y directions
x,y	Cartesian-coordinates
X,Y	Non dimensional coordinates
<i>Greek symbols</i>	
ρ	Fluid density, kgm^{-3}
α	Coefficient of Thermal diffusivity, m^2s^{-1}

β	Coefficient of Thermal expansion, K^{-1}
K	Medium Permeability
ϕ	Stream function

Introduction

Natural convection is very significant heat transfer mechanism for many engineering applications. Forced convection uses fans or pumps to supply the forces required to produce fluid motion, whereas natural convection relies entirely on fluid motion created by effects of buoyancy again, this result from density differences in the fluid caused by temperature gradients. It is an unconventional approach toward passive heat transfer for scenarios where active cooling inefficiencies or non-feasibility rule out its applicability, including electronic cooling, ventilation of buildings, and even safety critical systems in nuclear reactors. Electronic cooling as the application name itself, exemplifies that process of natural convection to remove heat by parts such as processors which could degrade its performance and lifetime.

This makes the natural convection heat transfer over porous media significantly important since it is due to its bigger effective surface area heating coupled with promoting fluid flow inside interconnected pores of the material. Natural convection occurs in fluid movement because of a density gradient initiated by a temperature difference. The presence of a porous medium also aids in enhancing fluid intrusion through the material, which increases heat transfer rates.

Porous materials are used in a broad spectrum of applications from insulation, electronics cooling, geothermal systems and nuclear reactors. The porous structure of these systems provides superior thermal conductivity for the efficient dissipation of heat. Improvement in thermal management with enhanced energy efficiency and performance-oriented design for enhancement in heat transfer systems by optimized structure as well as properties of porous media to be utilized in advanced applications of engineering.

Aleshkova & Sheremet [1] discussed unsteady natural convection within a square enclosure filled with a porous medium. Here, heat transfer characteristics are dependent on the porous medium properties along with time dependency. Bhowmick et al. [2] presented some investigation on the impacts of magnetic fields on the natural convection heat transfer from some embedded cylinders in porous enclosures, where it was found that magnetic fields can contribute an impact significantly with regard to the change in the rate of heat transfer. Ganapathy [3] Investigated the time-dependent convection in an infinite porous medium under the action of a heated sphere, and proved the fact that the nature of convection and rates of heat transfer depend on the temperature and time of the sphere.

Narasimhan & Reddy [4] Investigated the natural convection in the enclosure of the bidisperse porous medium. The authors have also concluded the fact that thermal as well as flow behavior is dependent upon the porosity distribution. Varol et al. [5] Analyzes two-dimensional natural convection in a

triangular porous enclosure, with an included square body, where this paper indicates that the shape and position of the embedded body affect the patterns of convection. Olayemi et al. [6] Natural convection heat transfer from an inclined rectangular cylinder in square enclosures presents both the orientation angle of the inclination and the size of the cylinder significantly affect the heat transfer. Iyi & Hasan [7] Studied natural convection flow in enclosures with staggered blockages, thus showing that there does exist a particular arrangement of blockages influencing the patterns of flow and further effect in heat transfer.

Ataei-Dadavi et al. [8] Conducted an experimental study about a differentially heated cavity filled with coarse porous media that proved the complex interplay in between the heating pattern and the porous media. Nammi et al. [9] Examines natural convection in a square porous enclosure with four heated cylinders and proves that the location at which the cylinders stand and, of course, the thermal condition significantly affects the overall heat transfer performance. Khanafer & Vafai [10]. Exposing the impact of a circular cylinder and flexible wall on the heat transfer by natural convection in a porous cavity, it was observed that changes in the shape of the cylinder with the alteration of wall flexibility would vary the heat transfer characteristics.

Bhowmick et al. [11] Heat transfer and entropy generation analysis for different geometries of heated cylinders in a non-uniformly heated enclosure that exhibits much variation with the shape of the cylinder and wall temperatures. Rasheed & Hasan [12] Effects of orientation on the natural convection heat transfer from heated triangular prism in porous media, which clearly shows orientation affects much the rates of heat transfers. Barman & Rao, [13]. Natural convection phenomenon in a wavy porous cavity has been demonstrated with an obstacle placed at its middle under the insulation process. Changes in the geometrical shapes of the cavities and the location of the obstacles are observed to influence the convection characteristics. Mercier et al. [14] The author discusses the behavior of natural convection within a partially porous cavity, and studies porosity as well as the geometry of the cavity toward the heat transfer.

Nouanegou et al. [15] Natural convection coupled with conduction and radiation in an inclined square enclosure was analyzed and proved to be of such a nature that both inclination and boundary conditions are dependent upon the rate of heat transfer. More, Shih et al. [16-17] He proves that the rotation of the cylinder has an influence on the pattern of fluid motion and also the patterns of heat transfer. Checks Periodical fluid flow and heat transfer in a square cavity by an insulated or isothermal rotating rectangular object, which depicts the effect of shape and rotation of an object on heat transfer. Ushachew et al. [18] It discusses natural convection in micropolar nanofluids with porous medium filled enclosure and variously embedded geometries that illustrate how the geometry of an object affects the heat transfer of the nanofluid. Bhowmick et al. [19] Found from two Examines the effects of magnetic field on the natural convection process due to cylinders that are placed within the porous enclosures. In both scenarios, it had to do with how the magnetic field was impacting the rate of heat transfer.

Basak et al. [20] Various researches have been conducted on natural convection in a square cavity containing porous medium, subject to various thermal boundary conditions, and it was concluded that the boundary conditions have pronounced effects on heat transfer performances. Nagaraju [21] Analyzes the heat and mass transfer problem in saturated porous media: one provides insight into basic behavior of heat and mass transfer in such media. Mishra & Chhabra, [22] Analysis of Natural Convection in Power-Law

Fluids from Differentially Heated Horizontal Cylinders under a Square Enclosure. Fluid properties and cylinder arrangement affect the transfer process.

Mahmood et al. [23] Research on CFD Simulations of Natural Convection from a Horizontal Cylinder in a Square Enclosure by Detailed Simulation Results on Heat Transfer Characteristics. Chen et al. [24] Conjugate Natural Convection Heat Transfer in an Open-ended Square Cavity Partially Filled with Porous Media an Effect of Porous Media on the Efficiency of Convection. Hussain & Hussein [25] Natural Convection Inside the Circular Cylinder Placed inside the Square Enclosure in Various Vertical Locations, position affects patterns of convection and transfer.

Tong and Subramanian [26] explored natural convection in partially porous media filled rectangular enclosures. The consequence was the weakening of convective currents and, consequently, heat transfer rates by the presence of the porous material. Aly [27] extended this work to a nanofluid-filled circular enclosure where porous media studies showed that nanofluids are excellent heat transfer enhancers. Oztop, Varol, and Pop [28] investigated triangular enclosures consisting of porous media and water close to 4°C and exhibited how geometry of the enclosure and thermal properties of water determine convection flows.

Baytaş and Pop [29] did special exploration on natural convection within trapezoidal enclosures and proved that the shape of the trapezoidal enclosures exerts influence over heat transfer due to alteration in convective flow. Moreover, Varol, Oztop, and Pop [30] established that the same square cavities divided diagonally containing porous media have asymmetric flow patterns and augment heat transfer as well.

Baytaş [31] examines thermal non-equilibrium in porous enclosures with emphasis on the impact of the interaction between conduction and convection in heat-generating solid phases on heat transfer. Solomon et al. [32] have made an experimental study on the influence of aspect ratios in square cavities filled with Al₂O₃-water nanofluids. As per their discussion, higher aspect ratios enhance heat transfer. Sheikholeslami et al. [33], has done a study on natural convection in an enclosure containing nanofluid having an elliptic inner cylinder. According to the discussion, the shape of the cylinder will be considerable while considering the convective flow and heat transfer.

Karimdoost Yasuri et al. [34] investigated magnetic field effects on natural convection and suppressed convective currents, accordingly heat transfer within square enclosures filled with nanofluid. Further, Ho et al. reported that alumina-water nanofluids enhance the heat transfer inside vertical square enclosures and confirmed the superior thermal properties of nanofluids. For example, Garbadeen et al. [35] showed that MWCNT-water nanofluids improved the heat transfer in square enclosures, and thus nanofluids can be a potential alternative for thermal management.

Boulaiah et al. and Mohebbi et al. [36] studied the arrangement of obstacles and heat sources inside enclosures, respectively, by using various geometries of obstacle and the various positions of heat source inside enclosures. The study of Boulaiah [37] on square enclosures containing cold inner obstacles indicated that the placement of obstacles affects heat transfer. Mohebbi's [38] study on nanofluid-filled C-shaped enclosures reveals that convection is affected by the position of the heat source. Cho et al. [39] discussed the analysis of natural convection in square enclosures containing hot elliptical cylinders and concluded that heat transfer depends on various aspect ratios of the cylinders. Charreh et al. [40] performed a numerical study on the subject of magnetohydrodynamic natural convection in porous square

cavities containing four embedded cylinders to present how magnetic fields and cylinder placement influence entropy generation and heat transfer behavior. Finally, Karimi et al. [41] numerically investigated unsteady natural convection from heated horizontal circular cylinders placed inside a square enclosure through their numerical simulation. Most of their work was focused on the transient flow patterns and thermal behavior under different configurations and boundary conditions, by which they presented valuable new insights into mechanisms of heat transfer.

Methodology

Considering is a square enclosure with side length 1m, and inside of it there are two Micro-Nuclear-Reactors. distance between the Micro-Nuclear-Reactors is given by S, values of it are within the range of $0.1 \leq S \leq 0.4$. Walls of the enclosure and Micro-Nuclear-Reactors are kept at constant temperature T_h , whereas there exists a wall of the enclosure whose temperature T_c is smaller than that of the Micro-Nuclear-Reactors, and during the analysis it is taken constant. The medium in the enclosure is regarded as a saturated Newtonian porous medium. Fluid properties are assumed constant, except for density. Density in this model is accounted for using the Boussinesq approximation.

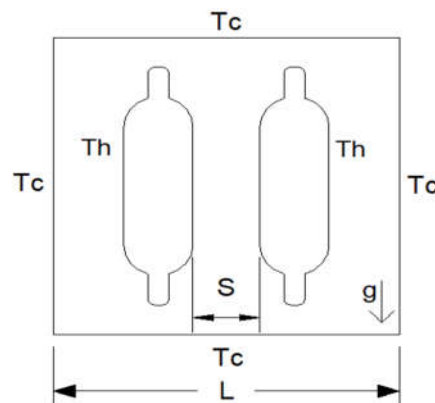


Fig.1: Schematic representation of the problem statement

Governing Equations

Flow in the enclosure is assumed to be two-dimensional, incompressible, and laminar. Non-dimensional governing equations are the mass conservation, momentum in both the x-and y-direction, and energy may be given as follows

1. Mass Conservation (Continuity Equation):

$$\frac{\partial U^*}{\partial X^*} + \frac{\partial V^*}{\partial Y^*} = 0 \quad (1)$$

2. Momentum Conservation in the x-direction:

$$\frac{\partial U^*}{\partial t^*} + U^* \frac{\partial U^*}{\partial X^*} + V^* \frac{\partial U^*}{\partial Y^*} = -\frac{\partial P^*}{\partial X^*} + \text{Pr} \left(\frac{\partial^2 U^*}{\partial X^{*2}} + \frac{\partial^2 U^*}{\partial Y^{*2}} \right) - \text{Pr} \frac{U}{\text{Da}} \quad (2)$$

3. Momentum Conservation in the y-direction:

$$\frac{\partial V^*}{\partial t^*} + U^* \frac{\partial V^*}{\partial X^*} + V^* \frac{\partial V^*}{\partial Y^*} = -\frac{\partial P^*}{\partial Y^*} + \text{Pr} \left(\frac{\partial^2 V^*}{\partial X^{*2}} + \frac{\partial^2 V^*}{\partial Y^{*2}} \right) - \text{Pr} \frac{V}{\text{Da}} + \text{RaPr}\theta^* \quad (3)$$

4. Energy Conservation:

$$\frac{\partial \theta^*}{\partial t^*} + U^* \frac{\partial \theta^*}{\partial X^*} + V^* \frac{\partial \theta^*}{\partial Y^*} = \left(\frac{\partial^2 \theta^*}{\partial X^{*2}} + \frac{\partial^2 \theta^*}{\partial Y^{*2}} \right) \quad (4)$$

Non-Dimensional Parameters:

The dimensionless quantities and parameters used in the above equations are expressed as

$$X^* = \frac{x}{L'}, Y^* = \frac{y}{L'}, t^* = \frac{at}{L^2}, U^* = \frac{uL}{\alpha}, V^* = \frac{vL}{\alpha}, P^* = \frac{pL^2}{\rho\alpha^2}, \theta^* = \frac{T-T_c}{T_h-T_c}, Da = \frac{k}{L^2}, Pr = \frac{\nu}{\alpha}, Ra = \frac{\beta g L^3 (T_h - T_c) Pr}{\nu^2}$$

There are x and y representations of the Cartesian coordinates here, which are fairly obvious horizontal and vertical directions, respectively. u and v are the corresponding velocity components. t denotes time, while α denotes thermal diffusivity, ν represents kinematic viscosity, ρ is the fluid density, p is pressure, k is permeability, and β is the thermal expansion coefficient. Key parameters that have been introduced are Rayleigh number (Ra), Prandtl number (Pr), and Darcy number (Da).

Boundary Conditions:

The boundary conditions applicable to the governing equations (1)-(4) are described as follows

- On the Micro-Nuclear-Reactors surfaces:

$$U^*=0, V^*=0, \theta^*=1, U^*=0, V^*=0, \theta^*=1 \quad (5)$$

- At the enclosure walls:

$$U^*=0, V^*=0, \theta^*=0, U^*=0, V^*=0, \theta^*=0 \quad (6)$$

Initial Conditions:

The initial conditions for the simulation assume atmospheric pressure across the entire domain. Other initial values used are

$$U^*=0, V^*=0, \theta^*=0 \text{ at } t^*=0 \quad (7)$$

Validation

We were justifying the correctness of the numerical scheme adopted to solve the governing transfer equations before stepping forward with parametric numerical runs. As such, Karimi et al. [41] have explored comparable parameters in his work on the porous cavity. The relative fluctuations of Nut

with distance S for the count of undulations diameter $d=0.2$ and for $Pr=0.7$, variation of Rayleigh number from 10^3 to 10^6 were compared. As illustrated in Figure1, the existing numerical simulation result is compared with the result established by Karimi et al. [41]

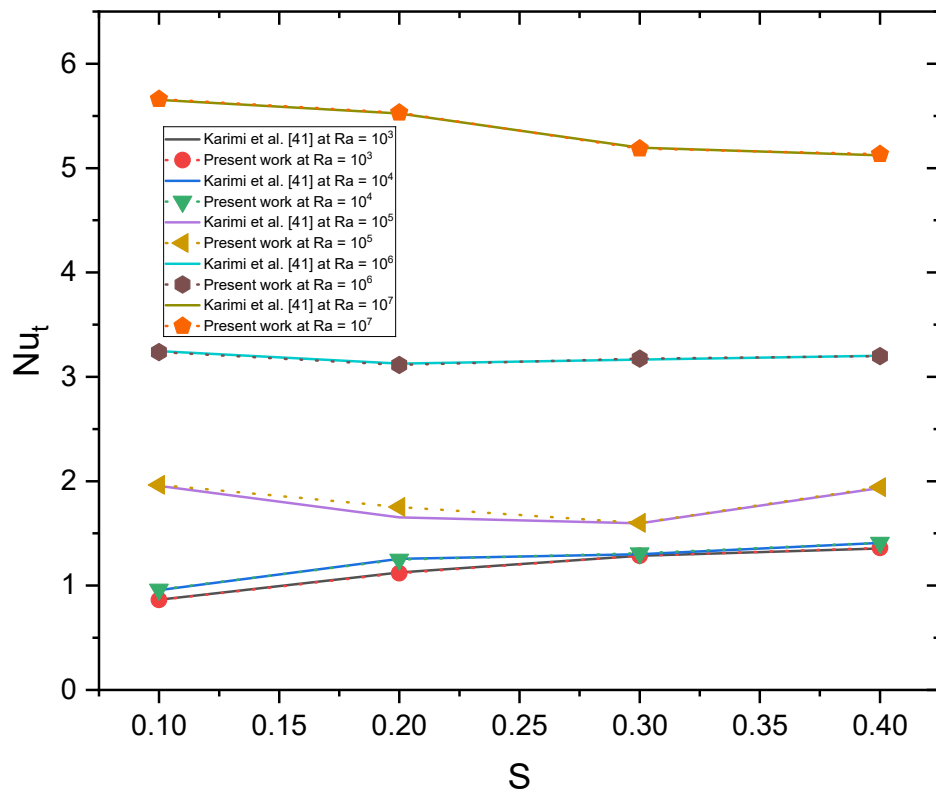


Fig.1: Validation of Nusselt number Nu_t variation with respect to Distance S at $10^3 \leq Ra \leq 10^7$ between Present work and Karimi et al.[41]

Results and Discussions

The complete results of natural convection heat transfer within a square enclosure, which is filled with porous medium, and containing two embedded Micro-Nuclear Reactors (Micro-Nuclear-Reactors) yield in the present analysis. Variation in distances between reactors to be (distance $S=0.1, 0.2, 0.3, 0.4$) on the other hand, the Rayleigh numbers were considered in the range of ($10^3 \leq Ra \leq 10^6$). Interactions of Darcy numbers as proposed in the range of $10^{-4} \leq Da \leq 10^{-2}$ were also explored by the study and also done the same numerical analysis setup using air medium for the Rayleigh numbers were considered in the range of ($10^3 \leq Ra \leq 10^6$). Critical attention is focused on the flow patterns-streamlines, temperature distribution-isotherms, and numerical heat transfer in terms of Nusselt number.

1. Rayleigh number and distance effect on flow patterns or streamlines:

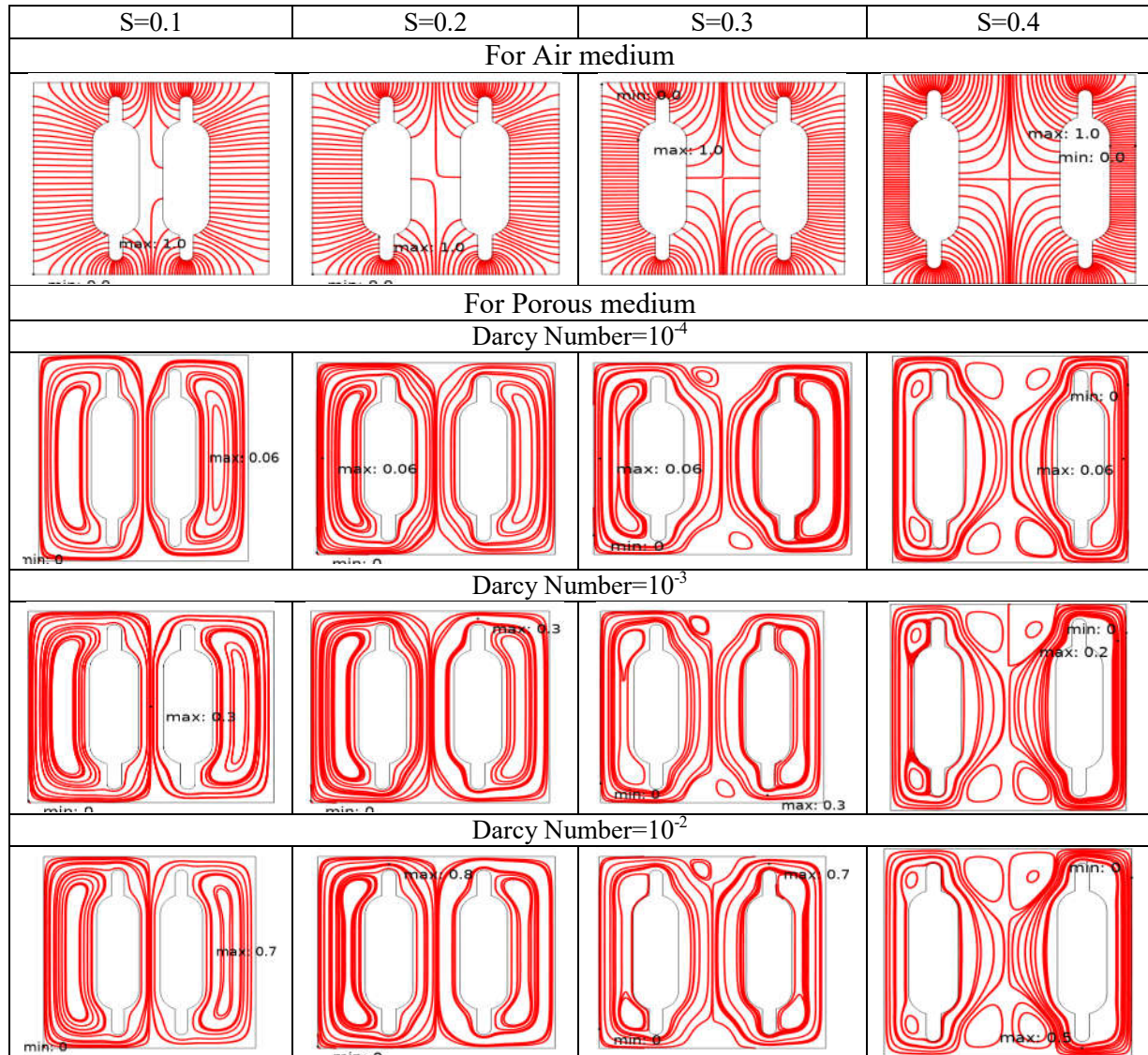


Fig.2: Streamlines for air medium and porous medium at different Darcy Numbers and at different distance(S) at Rayleigh Numbers (Ra)= 10^3

At Rayleigh number $Ra=10^3$, Fig.2 illustrates the proximity between the reactors at distance $S=0.1$ limits the formation of independent convective cells and the flow remains weak. In the air medium, the maximum value of the streamline function is $\phi = 1$, which shows the flow is mainly conduction dominated. The porosity within the medium results in the lower fluid stream function values, $\phi = 0.06$ for $Da = 10^{-4}$, $\phi = 0.3$ for $Da = 10^{-3}$, and $\phi = 0.7$ for $Da = 10^{-2}$. Such low values show that at such a low Ra , conduction is still the predominant mode of heat transfer. At distance $S=0.2$ again presents the same situation, and the streamline function remains maximum with a value of $\phi = 1$ in air. In porous medium values are also comparable to those obtained at distance $S=0.1$: with $\phi = 0.06$ for $Da = 10^{-4}$, $\phi = 0.3$ for Da

$= 10^{-3}$ and $\phi = 0.8$ for $Da = 10^{-2}$. A small rise in the values of streamlines in porous medium at $Da = 10^{-2}$ depicts a slight influence of permeability, but still, the mechanism of conduction is predominant. At distance $S=0.3$ the reactors are sufficiently far apart that the convective cells could be possible, yet still very weak. For the medium air, the streamline function is $\phi = 1$, and in the porous medium, it is very low: $\phi = 0.06$ for $Da = 10^{-4}$, $\phi = 0.3$ for $Da = 10^{-3}$ and $\phi = 0.7$ for $Da = 10^{-2}$. Once more, these once more agree with pure conduction flow, though the spacing has now increased. At distance $S=0.4$ the distance is large enough that the reactors act almost independently. In the air medium, the streamline function remains $\phi = 1$, while in the porous medium, the streamline values are still low at $\phi = 0.06$ for $Da = 10^{-4}$, $\phi = 0.2$ for $Da = 10^{-3}$, and $\phi = 0.5$ for $Da = 10^{-2}$. Therefore, once again, it has confirmed that for low Ra , the mechanism of heat transfer is dominated through conduction and convection takes the secondary role in the porous medium. The convection is weak, hence the streamlines are mostly smooth and circular. In the case of an increased Da value to 10^{-2} , the streamlines begin to exhibit a curvature but remain quite restricted by the small Ra .

At Rayleigh number $Ra=10^4$, Fig.3 illustrates, the Buoyancy forces are enhanced, supporting the convection cells. At distance $S=0.1$, the value of the stream function in the air medium remains at rest being equal to $\phi = 1$, but the flow becomes much better structured. For example, the corresponding values for the streamline function increase in porous medium: $\phi = 0.6$ by $Da = 10^{-4}$, $\phi = 3$ by $Da = 10^{-3}$, and $\phi = 7$ at $Da = 10^{-2}$. Therefore, an increase in the Rayleigh number leads to a certain enhancement of the role of convection in heat transfer, especially at large Darcy numbers. At distance $S=0.2$, more discrete convective cells are formed because of the greater distance of the reactors. In the air medium, the values of the streamline function remain to be $\phi = 1$, while for the porous medium, the values are increased up to $\phi = 0.6$ at $Da = 10^{-4}$, $\phi = 3$ at $Da = 10^{-3}$ and at $Da = 10^{-2}$, the value is increased up to $\phi = 8$. Higher values of the streamline function depict that with Da , the porous medium is becoming more penetrable for the convective flow. At distance $S=0.3$ is the ideal distance between the reactors gives a better formation of the convective cells. In the air medium, the value of the streamline function is $\phi = 1$, and in the porous medium, $\phi = 0.6$ when $Da = 10^{-4}$, $\phi = 3$ at $Da = 10^{-3}$, and $\phi = 7$ at $Da = 10^{-2}$. This unequivocally points out that even at moderate values of Da , at higher values of Ra 's, the porous medium supports more significant convective flow. At distance $S=0.4$ the reactors are spaced far apart, and the convective cells work almost independently. Streamlines in the air medium take the values of $\phi = 1$ and in the porous medium $\phi = 0.6$ for $Da = 10^{-4}$, $\phi = 2$ for $Da = 10^{-3}$, and $\phi = 5$ for $Da = 10^{-2}$. Though a convective flow is more powerful than when $Ra = 10^3$, it is complicated by a large distance between the reactors, thus hindering interaction growth between the convective cells of the reactors.

At $Ra = 10^4$ buoyancy forces are quite stronger and the forming of convective cells will be more definite. As one proceeds to the air medium, streamline patterns around each reactor become much apparent. As the gap stretches up to $S=0.3$ and even further to $S=0.4$, you would have more distinct convective cells forming individually around each reactor. In the porous medium, the streamlines still reflect resistance to flow but are significantly more curved as Da increases. For $Da = 10^{-2}$, the flow is far stronger than for $Da = 10^{-4}$, and the convective cells appear here to be more distinct, although they are even weaker than in the air medium.

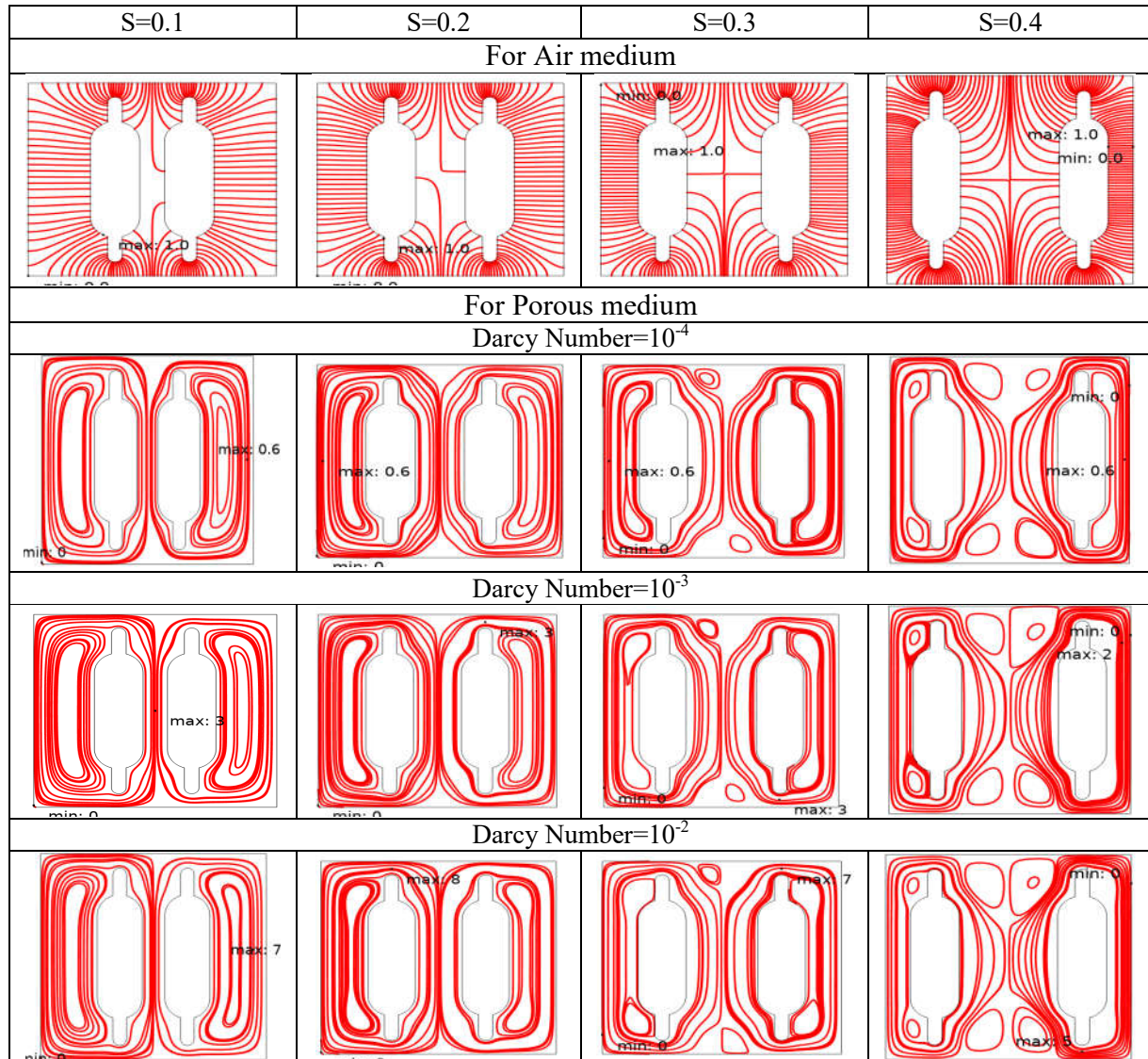
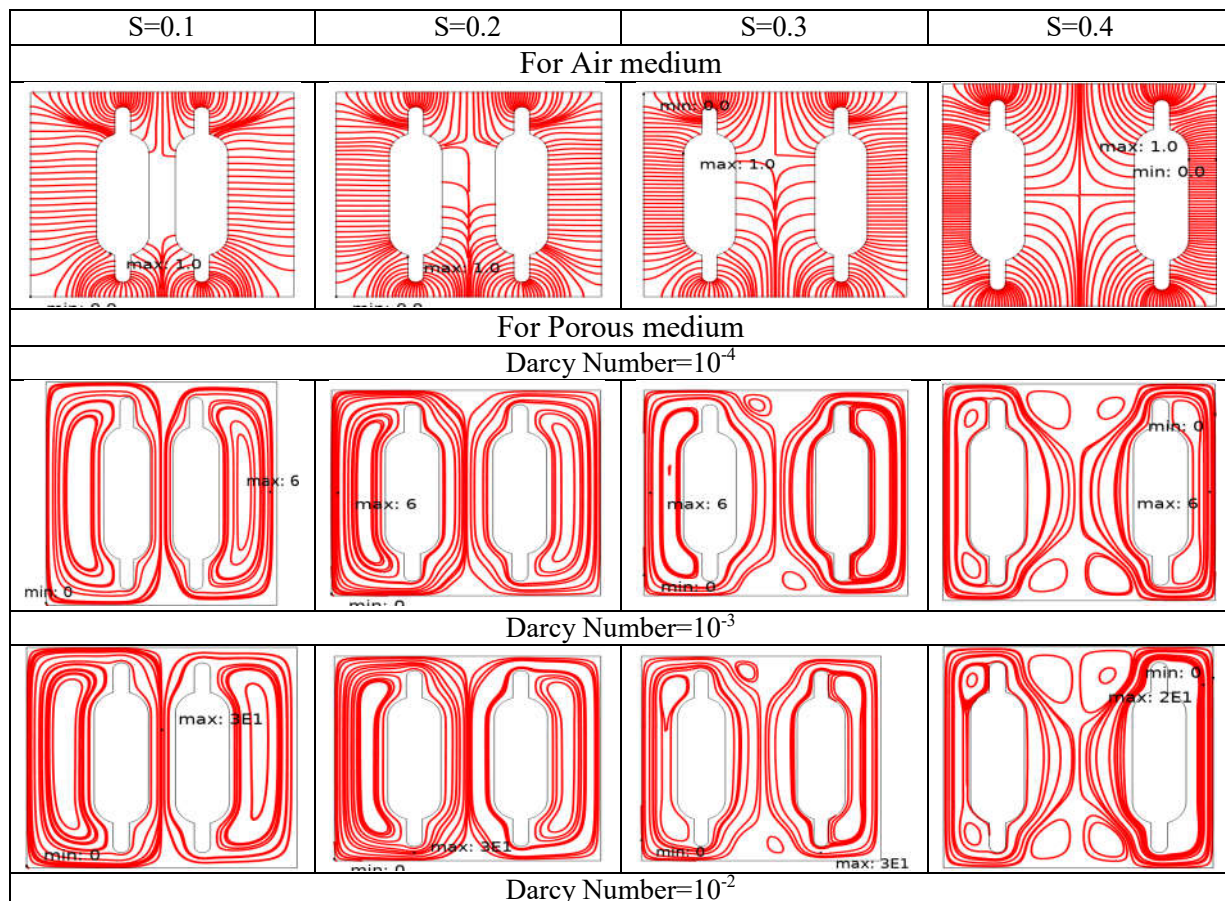


Fig.3: Streamlines for air medium and porous medium at different Darcy Numbers and at different distance(S) at Rayleigh Numbers $Ra=10^4$

At Rayleigh number $Ra=10^5$ Fig.4 illustrates, buoyancy forces dominate and the convective currents are more dominant. At distance $S=0.1$ the streamline function value is still at $\phi=1$ for the air medium but with dramatically improved flows. As was also the case for the porous medium, streamline function values are significantly higher at $\phi=6$ for $Da=10^{-4}$, at $\phi=30$ for $Da=10^{-3}$ and at $\phi=70$ for $Da=10^{-2}$. The above values show that convection becomes more important with increasing porosity within the porous medium. At distance $S=0.2$ spacing increases the convective currents the stronger. For air medium, ϕ becomes equal to 1, while for porous medium ϕ becomes equal to 6 for $Da=10^{-4}$, ϕ equal to 30 for ϕ

$Da = 10^{-3}$, and $\phi =$ equal to 80 for $Da = 10^{-2}$. More values of the streamline mean that when a greater distance is used, convection grows more effective when larger values of Da are used. At distance $S=0.3$ the distance at which convection is optimum, and at this distance, the streamline function in the air medium remains the same as $\phi = 1$ whereas in the porous medium, the values go up to $\phi = 6$ at $Da = 10^{-4}$, $\phi = 30$ at $Da = 10^{-3}$, and $\phi = 70$ at $Da = 10^{-2}$. That means at higher values of Ra and Da , the porous medium facilitates fully developed convective cells and hence transfers heat better. At distance $S=0.4$ there is an increased distance decreases contact between the convective fields of the reactor. Meanwhile, in the air medium, $\phi = 1$, and values for ϕ in the porous medium are as follows: $\phi = 6$ at $Da = 10^{-4}$, $\phi = 20$ at $Da = 10^{-3}$, and $\phi = 50$ at $Da = 10^{-2}$. Convection flows do not disappear but the growth of distance decreases in the general strength of convective currents.

At $Ra = 10^5$, convection overtakes the dominant mechanism of heat transfer, and strong curved patterns along with vortices in the air medium show around the reactors. At $Da = 10^{-2}$, the flow within the porous medium is still constricted, and the streamlines display tighter curvature and thus greater strength of convective currents. At $Da = 10^{-2}$, the flow within the porous medium is still constricted, and the streamlines display tighter curvature and thus greater strength of convective currents. However, the porous structure continues to damp the flow intensity compared to that in an air medium.



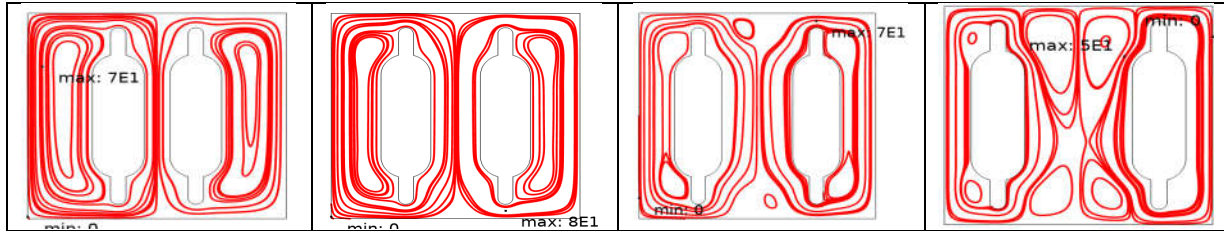


Fig.4: Streamlines for air medium and porous medium at different Darcy Numbers at different distance(S) at Rayleigh Numbers (Ra)= 10^5

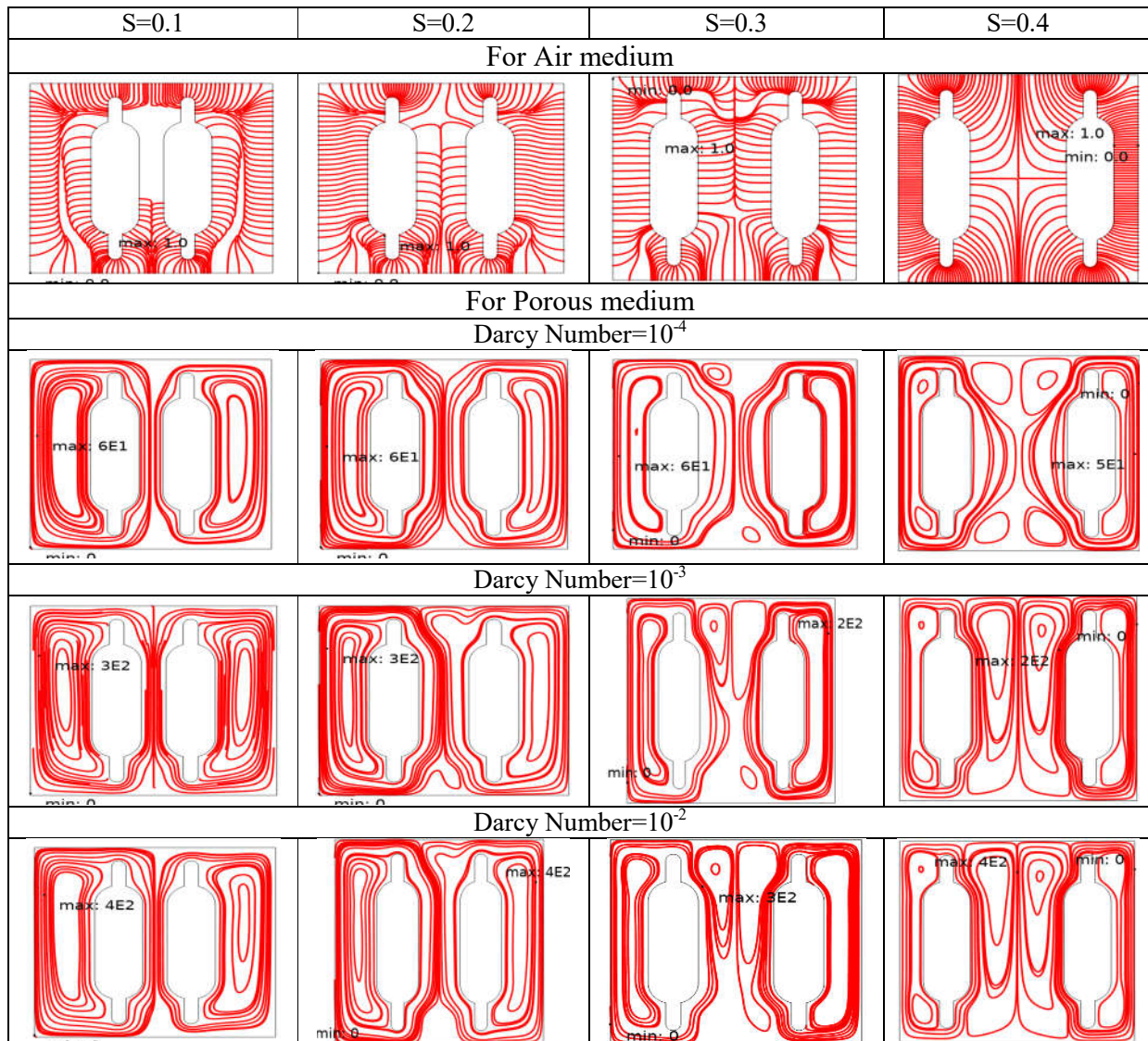


Fig.5: Streamlines for air medium and porous medium at different Darcy Numbers and t different distance(S) at Rayleigh Numbers (Ra)= 10^6

At Rayleigh number $Ra=10^6$ Fig.5 illustrates, the buoyancy forces are maximum and convection dominates the process of heat transfer. At distance $S=0.1$ the air medium attains the maximum streamline function value of $\phi = 1$, whereas the porous medium shoots up sharply to very large values of $\phi = 60$ for

$Da = 10^{-4}$, $\phi = 300$ for $Da = 10^{-3}$ and $\phi = 700$ for $Da = 10^{-2}$. All these large values indicate that even at the closest spacing porous medium supports strong convection at high Ra and Da values. At distance $S=0.2$ the presence of fluid flow between the reactors raises the number of independent convective cells. At the porous medium, $\phi = 60$ at $Da = 10^{-4}$ and $\phi = 300$ when $Da = 10^{-3}$ and $\phi = 400$ at $Da = 10^{-2}$. The low values of $\phi = 400$ at $Da = 10^{-2}$ compared to distance $S=0.1$ indicate weak interaction of the convective cells. At distance $S=0.3$ the values for the values in the porous medium go up to $Da = 10^{-4}$ $\phi = 60$, $Da = 10^{-3}$ $\phi = 300$, and $Da = 10^{-2}$ $\phi = 700$. For the air medium, however, the value of the streamline function at the optimum distance for convection remains at $\phi = 1$. This confirms that at high Ra and Da values, convection is the dominant mode of heat transfer: and that the porous medium is no bar to fully developed convective currents. At distance $S=0.4$ the reactors are separated by a distance such that the convective cells of the reactors are well separated. For all cases in the air phase $\phi = 1$, and in the porous phase $\phi = 50$ at $Da = 10^{-4}$, $\phi = 200$ at $Da = 10^{-3}$, and $\phi = 400$ at $Da = 10^{-2}$. Although convection is still of major importance, the minimal interaction between the reactors restrains the total fluxes of convection.

At $Ra = 10^6$, the buoyancy forces are very strong, and the streamlines in the air medium portray intense swirling vortices. When $S=0.1$, the convective cells merge, resulting in highly curved and intense vortices that circulate rapidly around the reactors. With increases in s to 0.3 and $S=0.4$, the convective cells become fully developed and independent with large, elliptical and circular patterns and complex circulation. For $Da = 10^{-2}$, the flow remains similar in the porosity medium, nevertheless, resistance from the porous structure weakens the magnitudes of the streamlines as compared to those in the air medium.

2. Isotherms:

The isotherms inform us as to the temperature distribution within the cavity, thus depicting the isothermal regions. The shape and spacing of the isotherms let us know how the heat transfer is being balanced between conduction and convection. At high enough values of Ra and/or Da, the isotherms are distorted by the convective currents and their gradients become more pointed. Below we detail what is observed for the behavior of the isotherms at each distance, Ra, and Da.

At Rayleigh number $Ra=10^3$ Fig.6 illustrates, at distance $S=0.1$ isotherms are relatively smooth and evenly distributed both in the air and in the porous medium. I found the maximum and minimum isotherm function for air medium as $T_{\max}=1$ and $T_{\min}=0.04$. The isotherms inside the porous medium indicate that the main way of heat transfer has been conduction, and almost negligible distortion has been done by convection. I found the maximum and minimum isotherm function for porous medium as $T_{\max}=0.06$ and $T_{\min}=0.007$ at $Da=10^{-4}$, $T_{\max}=0.3$ and $T_{\min}=0.07$ at $Da=10^{-3}$, $T_{\max}=400$ and $T_{\min}=10$ at $Da=10^{-2}$. Isotherms for the porous medium are even smoother in comparison because the porous medium tends to resist any fluid flow. In this case, the temperature distribution is still isothermal but with weak curvature when Da is increased. This corresponds to a weak convection. As Da increases up to 10^{-2} the distortion of isotherms slightly increases, yet it seems that conduction prevails. At distance $S=0.2$ the isotherms are again very similar to those at distance $S=0.1$. I found the maximum and minimum isotherm function for air medium as $T_{\max}=1$ and $T_{\min}=0.04$. And I found that the maximum and minimum isotherm function for porous medium as $T_{\max}=0.06$ and $T_{\min}=0.008$ at $Da=10^{-4}$, $T_{\max}=0.3$ and $T_{\min}=0.07$ at $Da=10^{-3}$, $T_{\max}=0.7$ and $T_{\min}=0.03$ at $Da=10^{-2}$. In the air medium the isotherms are again mainly undisturbed, and in the porous medium, only slightly more curved than at $Da = 10^{-2}$. Conduction, however again dominates the mechanism of heat transfer at this low value of Ra. At distance $S=0.3$ Both display intensely distorted

isotherms. In the air medium near the reactors, temperature gradients would be very pronounced. I found the maximum and minimum isotherm function for air medium as $T_{\max}=1$ and $T_{\min}=0.04$. Nevertheless, conduction prevails. In the porous medium, one might have expected that even for $Da = 10^{-2}$ the isotherms would still be as highly undistorted since the flow is so strongly impeded that little convection is produced. And I found that the maximum and minimum isotherm function for porous medium as $T_{\max}=0.06$ and $T_{\min}=0.008$ at $Da=10^{-4}$, $T_{\max}=0.3$ and $T_{\min}=0.09$ at $Da=10^{-3}$, $T_{\max}=0.7$ and $T_{\min}=0.09$ at $Da=10^{-2}$. At distance $S=0.4$ isotherms are fairly smooth and spread out, with a homogeneous temperature distribution both in the air and in the porous medium, except for slight curvatures in the near-wall regions of the reactors. I found the maximum and minimum isotherm function for air medium as $T_{\max}=1$ and $T_{\min}=0.04$. When $Da = 10^{-2}$, distortion in the isotherm is at its minimum, meaning that convection has not yet become a dominant mode to the heat transfer. And I found that the maximum and minimum isotherm function for porous medium as $T_{\max}=0.05$ and $T_{\min}=0.007$ at $Da=10^{-4}$, $T_{\max}=0.2$ and $T_{\min}=0.09$ at $Da=10^{-3}$, $T_{\max}=0.4$ and $T_{\min}=0.09$ at $Da=10^{-2}$.

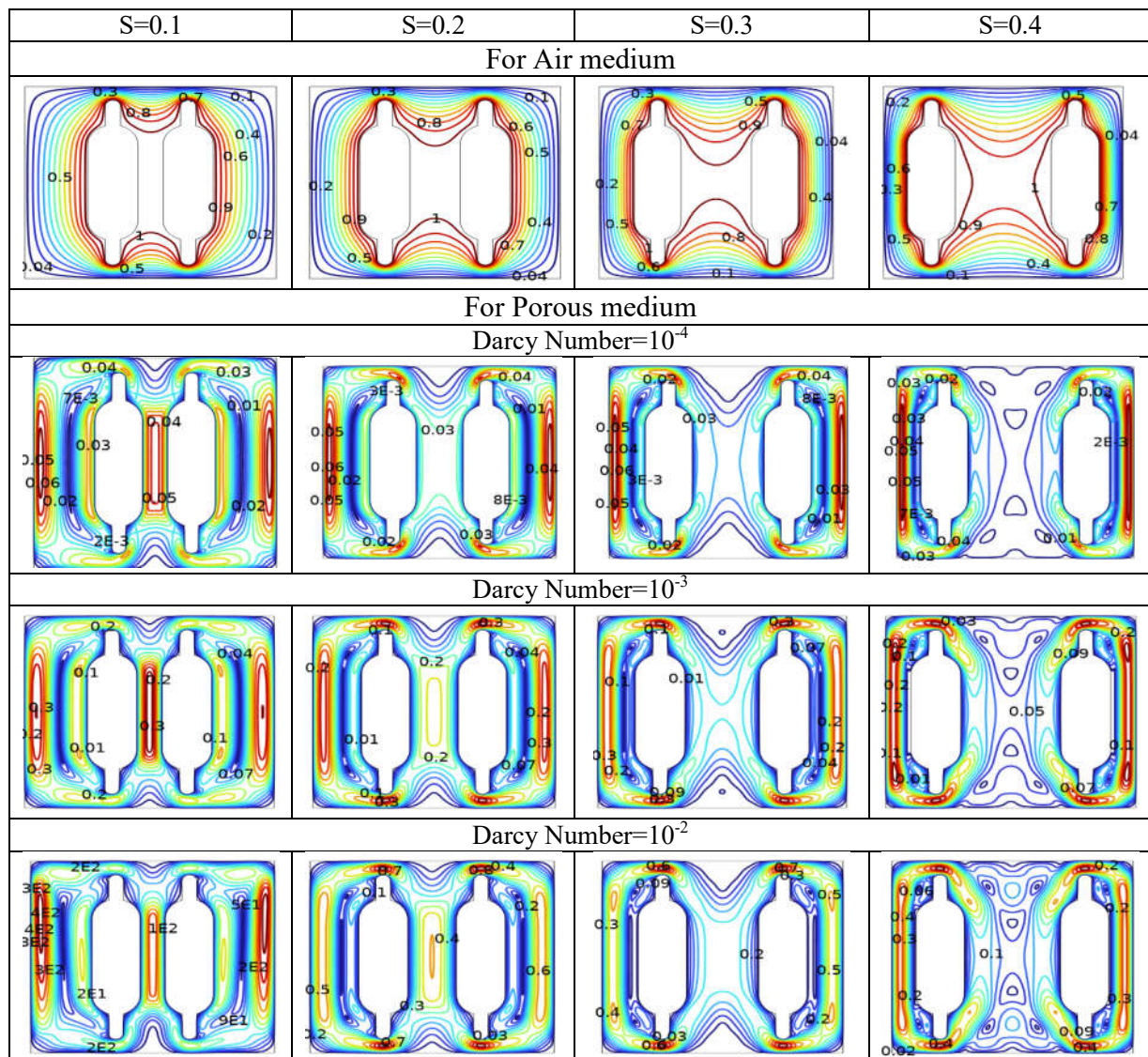


Fig.6: Isotherms for air medium and porous medium at different Darcy Numbers and at different distance(S) at Rayleigh Numbers (Ra)= 10^3

At Rayleigh number $Ra=10^4$ Fig.7 illustrates, the isotherms were more distorted and contribution from convection increased when a Rayleigh number of 10^4 was maintained. At distance $S=0.1$ isotherms in the air medium around the reactors are curved: there is the onset of convective heat transfer. I found the maximum and minimum isotherm function for air medium as $T_{\max}=1$ and $T_{\min}=0.04$. The temperature gradients around the reactors become much larger, but conduction is still a major mode of heat transfer for the porous medium. For the porous medium, the distortion of the isotherms was much stronger with higher values of Da , especially at $Da = 10^{-2}$. And I found that the maximum and minimum isotherm function for porous medium as $T_{\max}=0.6$ and $T_{\min}=0.07$ at $Da=10^{-4}$, $T_{\max}=3$ and $T_{\min}=0.7$ at $Da=10^{-3}$, $T_{\max}=300$ and $T_{\min}=10$

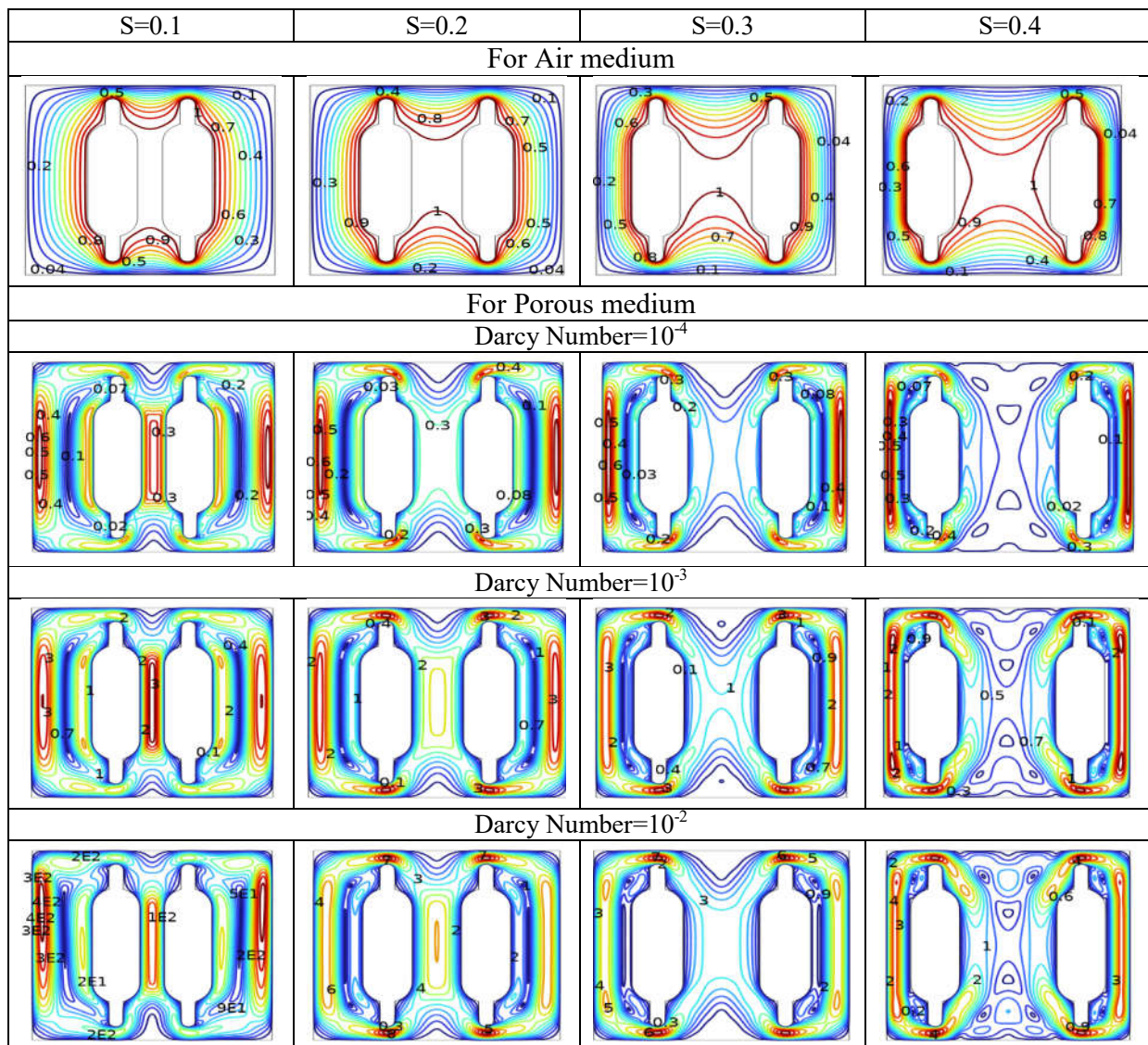
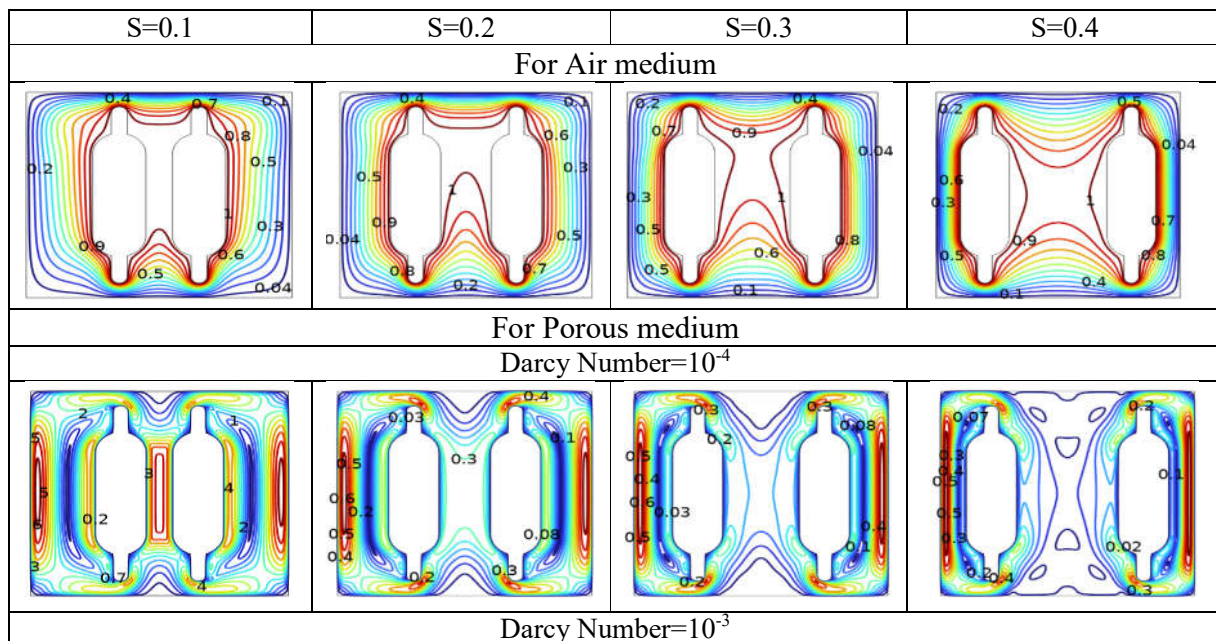


Fig.7: Isotherms for air medium and porous medium at different Darcy Numbers and at different distance(S) at Rayleigh Numbers (Ra)= 10^4

at $Da=10^{-2}$. This, of course, means that convective effects begin to play a role in the temperature fields. At distance $S=0.2$ both mediums have isotherms more curved than at distance $S=0.1$. I found the maximum and minimum isotherm function for air medium as $T_{\max}=1$ and $T_{\min}=0.04$. The steeper temperature gradients around the reactors in the case of the air medium lead to stronger convection. For $Da = 10^{-2}$, this medium has its isotherm distortion more pronounced, it means porosity of the structure begins to be sufficient for fluid flow through it and convective heat transfer is stronger. And I found that the maximum and minimum isotherm function for porous medium as $T_{\max}=0.6$ and $T_{\min}=0.08$ at $Da=10^{-4}$, $T_{\max}=3$ and $T_{\min}=0.7$ at $Da=10^{-3}$, $T_{\max}=7$ and $T_{\min}=0.3$ at $Da=10^{-2}$. At distance $S=0.3$ this spacing maximizes the distortion of the isotherm in both media, air and porous medium. I found the maximum and minimum isotherm function for air medium as $T_{\max}=1$ and $T_{\min}=0.04$. In the air medium, the isotherms are densely placed round the reactors, with steep temperature gradients and with a strong convective current. And I found that the maximum and minimum isotherm function for porous medium as $T_{\max}=0.6$ and $T_{\min}=0.08$ at $Da=10^{-4}$, $T_{\max}=3$ and $T_{\min}=0.7$ at $Da=10^{-3}$, $T_{\max}=7$ and $T_{\min}=0.3$ at $Da=10^{-2}$. In the porous medium, distortions are especially larger for $Da = 10^{-2}$ meaning that convection tends to play a more important role in the transfer as the distance between reactors becomes larger. At distance $S=0.4$ The isotherms appear to be much more localized around each reactor, indicating that the convective cells are not interacting with each other. In the air medium, isotherms are somewhat wavy in the reactors' areas, but convection does have an influence on heat transfer, however, it's not as strong at these distances. I found the maximum and minimum isotherm function for air medium as $T_{\max}=1$ and $T_{\min}=0.04$. In the porous medium, isotherms are still wavy when $Da = 10^{-2}$. However, the reduced inter-reaction between the reactors limits the convection's impact on the process as a whole. And I found that the maximum and minimum isotherm function for porous medium as $T_{\max}=0.5$ and $T_{\min}=0.07$ at $Da=10^{-4}$, $T_{\max}=2$ and $T_{\min}=0.7$ at $Da=10^{-3}$, $T_{\max}=4$ and $T_{\min}=0.6$ at $Da=10^{-2}$.



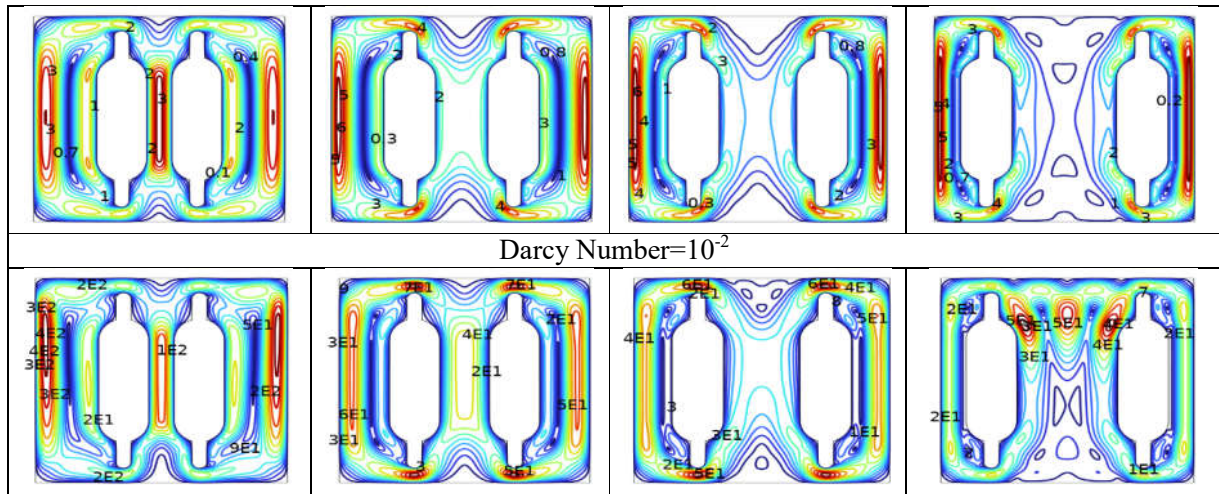
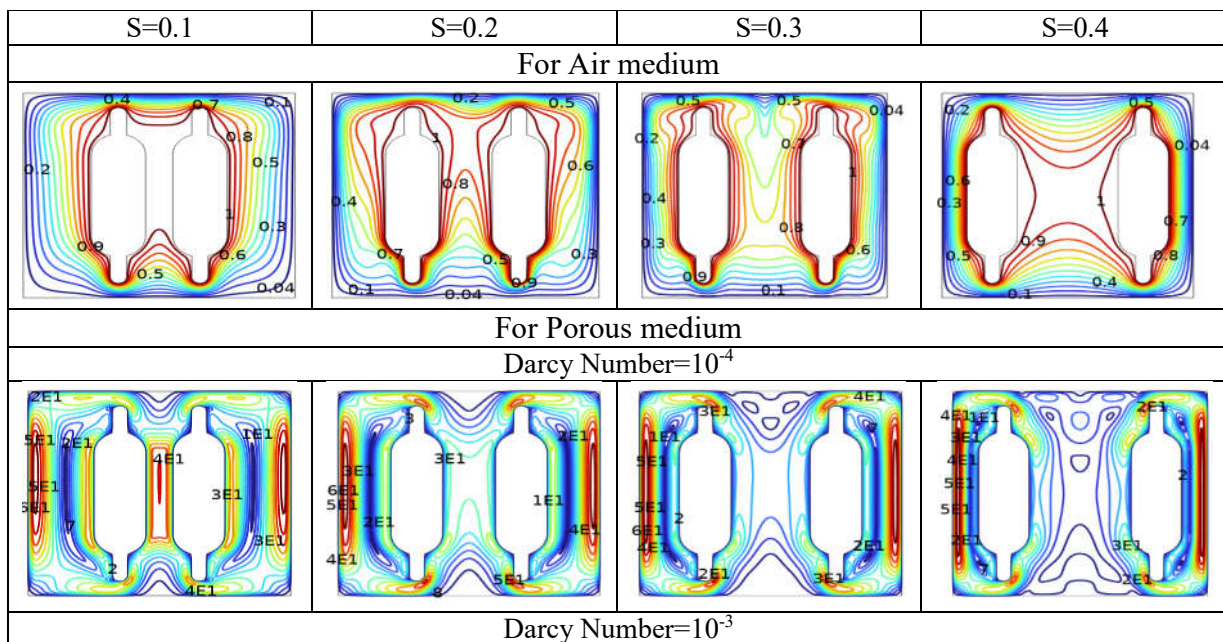


Fig.8: Isotherms for air medium and porous medium at different Darcy Numbers and at different distance(S) at Rayleigh Numbers (Ra)= 10^5

At Rayleigh number $Ra=10^5$ Fig.8, buoyancy forces are much stronger, convective currents dominate the convective heat transfer process. At distance $S=0.1$ the significant distortion of the isotherms in the air medium near the reactors indicates strong convection along with steep temperature gradients. I found the maximum and minimum isotherm function for air medium as $T_{\max}=1$ and $T_{\min}=0.04$. The increased curvature in the isotherms implies that heat is transferred more efficiently through convection. And I found that the maximum and minimum isotherm function for porous medium as $T_{\max}=6$ and $T_{\min}=0.7$ at $Da=10^{-4}$, $T_{\max}=3$ and $T_{\min}=0.7$ at $Da=10^{-3}$, $T_{\max}=400$ and $T_{\min}=10$ at $Da=10^{-2}$. Isotherms are strongly distorted at higher values of Da and considerably at $Da=10^{-2}$ brought about by the increase in permeability of the medium in the porous medium. At distance $S=0.2$ for both cases of media-in the air as well as porous media-the isotherms are more curved. The gradients of temperature in reactors with the medium of air are steep. I found the maximum and minimum isotherm function for air medium as $T_{\max}=1$ and $T_{\min}=0.04$. Isotherms show strong convective currents present in such media. And I found that the maximum and minimum isotherm function for porous medium as $T_{\max}=0.6$ and $T_{\min}=0.08$ at $Da=10^{-4}$, $T_{\max}=6$ and $T_{\min}=0.3$ at $Da=10^{-3}$, $T_{\max}=70$ and $T_{\min}=3$ at $Da=10^{-2}$. At $Da=10^{-2}$, isotherms are strongly distorted in the porous medium, this is because convection has now become leading mechanism of heat transfer as the porous medium became more permeable. At distance $S=0.3$ the isotherms of both media have large curvature with respect to both media, even more around the reactors. I found the maximum and minimum isotherm function for air medium as $T_{\max}=1$ and $T_{\min}=0.04$. In the air medium, closely packed isotherms near the reactors imply a steeper temperature gradient and an active convection. And I found that the maximum and minimum isotherm function for porous medium as $T_{\max}=0.6$ and $T_{\min}=0.08$ at $Da=10^{-4}$, $T_{\max}=6$ and $T_{\min}=0.3$ at $Da=10^{-3}$, $T_{\max}=60$ and $T_{\min}=3$ at $Da=10^{-2}$. In the porous medium, isotherms became highly distorted at $Da=10^{-2}$, thus, it validates the fact that convection is the mechanism of heat transport in this distance and Rayleigh number. At distance $S=0.4$ isotherms are more localized near each reactor but still distorted. I found the maximum and minimum isotherm function for air medium as $T_{\max}=1$ and $T_{\min}=0.04$. In the air medium, temperature gradients remain greater near the reactors and are due to strong convective currents though independence of the convective cells limits the convective heat transfer. I found that the maximum and minimum isotherm function for porous medium as $T_{\max}=0.5$ and $T_{\min}=0.07$ at $Da=10^{-4}$, $T_{\max}=5$ and $T_{\min}=0.7$ at $Da=10^{-3}$, $T_{\max}=50$ and $T_{\min}=2$ at $Da=10^{-2}$. In the porous

medium, even at $Da = 10^{-2}$, the isotherms are distorted though the reduced interaction between the reactors reduces the effects of convection.

At Rayleigh number $Ra=10^6$ Fig.9, the buoyancy forces are maximum in strength at $Ra = 10^6$, whereas convection completely dominates the process of heat transfer. At distance $S=0.1$ found the maximum and minimum isotherm function for air medium as $T_{\max}=1$ and $T_{\min}=0.04$. At $Da = 10^{-2}$, isotherms in the air medium turn to be tightly compressed in the reactor vicinity because of strong convective currents and steep temperature gradients, whereas at the same time, it is revealed that isotherms for the porous-medium are highly distorted as well that demonstrates convection dominating as the mechanism of heat transfer even within the porosity structure. And I found that the maximum and minimum isotherm function for porous medium as $T_{\max}=50$ and $T_{\min}=2$ at $Da=10^{-4}$, $T_{\max}=300$ and $T_{\min}=10$ at $Da=10^{-3}$, $T_{\max}=400$ and $T_{\min}=50$ at $Da=10^{-2}$. At distance $S=0.2$ isotherms in the both mediums are more distorted in reflecting stronger convective currents. I found the maximum and minimum isotherm function for air medium as $T_{\max}=1$ and $T_{\min}=0.04$. At the air medium, isotherms are closer packed around the reactors with sharp temperature gradients reflecting vigorous convection in that regime. And I found that the maximum and minimum isotherm function for porous medium as $T_{\max}=60$ and $T_{\min}=3$ at $Da=10^{-4}$, $T_{\max}=300$ and $T_{\min}=60$ at $Da=10^{-3}$, $T_{\max}=400$ and $T_{\min}=20$ at $Da=10^{-2}$. In the porous medium, isotherms at $Da = 10^{-2}$ are highly curved, which affirms that the porous medium is well permitting efficient convective heat transfer at that Ra value. At distance $S=0.3$ the isotherms in the air medium are highly distorted, with very strong temperature gradients near the reactors, so this predicts very strong convection. I found the maximum and minimum isotherm function for air medium as $T_{\max}=1$ and $T_{\min}=0.04$. Isotherms at $Da = 10^{-2}$ in the porous medium expose a high degree of curvature that confirms that, at this distance and Rayleigh number, the contribution of convection to the process of heat transfer is dominant I found that the maximum and minimum isotherm function for porous medium as $T_{\max}=50$ and $T_{\min}=2$ at $Da=10^{-4}$, $T_{\max}=200$ and $T_{\min}=7$ at $Da=10^{-3}$, $T_{\max}=200$ and $T_{\min}=40$ at $Da=10^{-2}$. In fact, this distance guarantees the most efficient heat transfer by convection as the cells appear well developed around each reactor. At distance $S=0.4$ although isotherms are distorted but still, the distance between reactors so large reduces the overall heat transfer.



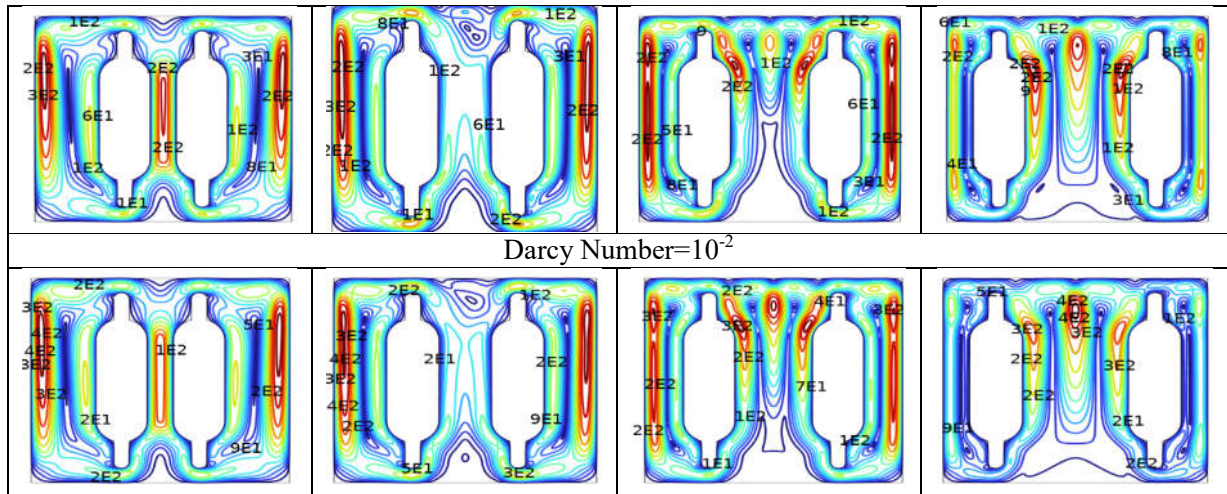
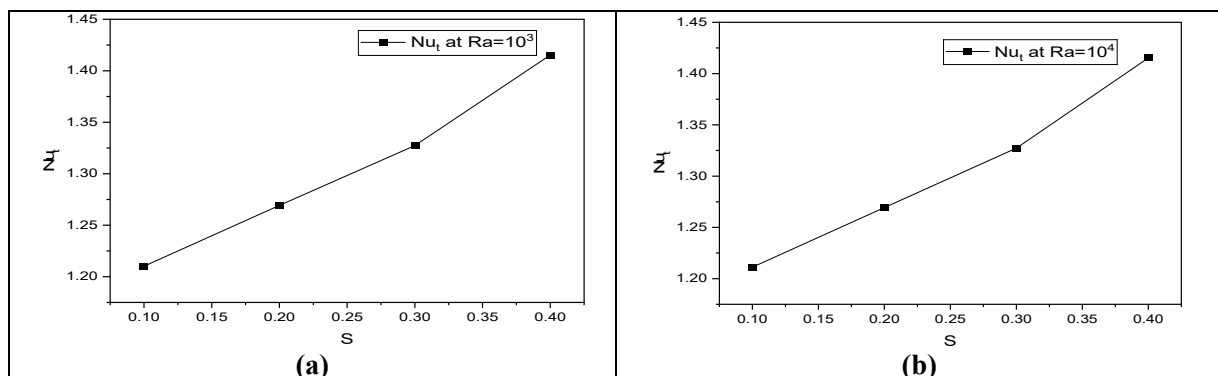


Fig.9: Isotherms for air medium and porous medium at different Darcy Numbers and at different distance(S) at Rayleigh Numbers (Ra)= 10^6

I found the maximum and minimum isotherm function for air medium as $T_{\max}=1$ and $T_{\min}=0.04$. Isotherms in the air medium near reactors really are curved, signifying that there is substantial convection. However, reduced interaction by the convective cells also limits the overall heat transfer. And I found that the maximum and minimum isotherm function for porous medium as $T_{\max}=50$ and $T_{\min}=2$ at $Da=10^{-4}$, $T_{\max}=200$ and $T_{\min}=9$ at $Da=10^{-3}$, $T_{\max}=400$ and $T_{\min}=20$ at $Da=10^{-2}$.

3.Nusselt Number:

The Nusselt number is very important in the analyses of heat transfer. This is specifically significant in relating the contribution of convection to conduction. Changes in Nu with changes in Rayleigh numbers, distances, and Darcy numbers may provide insight into how the system transitions from a regime dominated by conduction to a regime dominated by convection. Below shows in detail the percentage differences of Nu compared to Ra values ranging from 10^3 to 10^6 for both air and porous mediums at various distances describe how changes in buoyancy forces and permeability alter the heat transfer process.



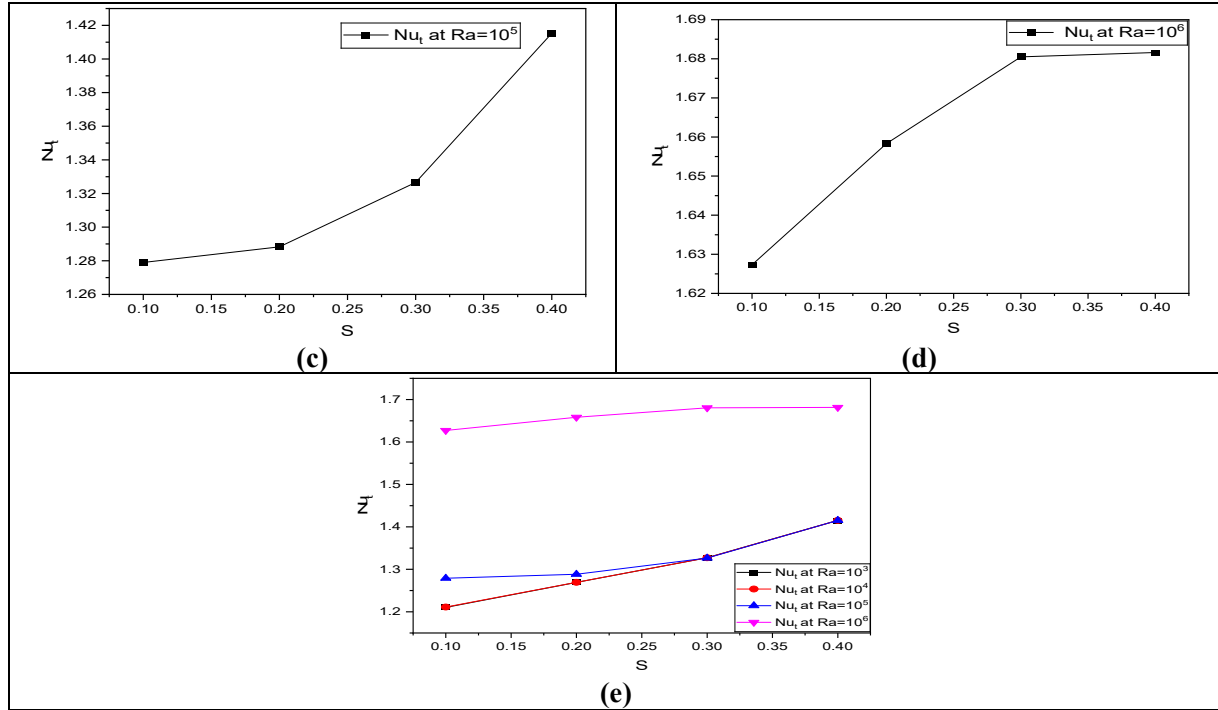


Fig.10: Spacing of Micro-Nuclear-Reactor (S) Vs Nusselt Number (Nu) at $10^3 \leq Ra \leq 10^6$ for air medium.

From Fig.10 Nusselt number of air medium varies reasonably with increase in Ra number at distance of reactor, $S = 0.1$. For the transition from $Ra = 10^3$ to $Ra = 10^4$, the Nusselt number increases by just 0.08%, and so at these lower Rayleigh numbers, the system is mainly conduction dominated with convection only beginning to be involved in transferring heat. But once Ra reaches 10^5 , it enhances the Nusselt number substantially to the tune of 5.6% and this signifies that convective currents start dominating. The Nusselt number increases sharply by 27.27% for a Ra of 10^6 , which strongly suggests overwhelming buoyancy-driven convection at this high Ra. The significant growth indicates that natural convection is a much more important mode of heat transfer, effectively enhancing heat transfer as the Rayleigh number increases.

For the case of the porous medium with $Da = 10^{-4}$ (Fig.11), the Nusselt number behavior is different. As in the Darcy number of Ra from 10^3 to 10^4 , Nu increases very slightly by 0.03%, which proves that convection has a negligible influence on this lower value of the Darcy number where the permeability is restricted. While raising Ra value to 10^5 , Nusselt number is seen to decrease by -0.32% and hence the porous structure proves to be an inhibitor for the fluid motion and convection process is restricted. This is further confirmed when Ra reaches 10^6 , where the Nusselt number decreases by -3.48%. This drop indicates that even at higher Ra, the low permeability of the porous medium severely restricts convective currents, and heat transfer remains relatively inefficient as compared with the air medium.

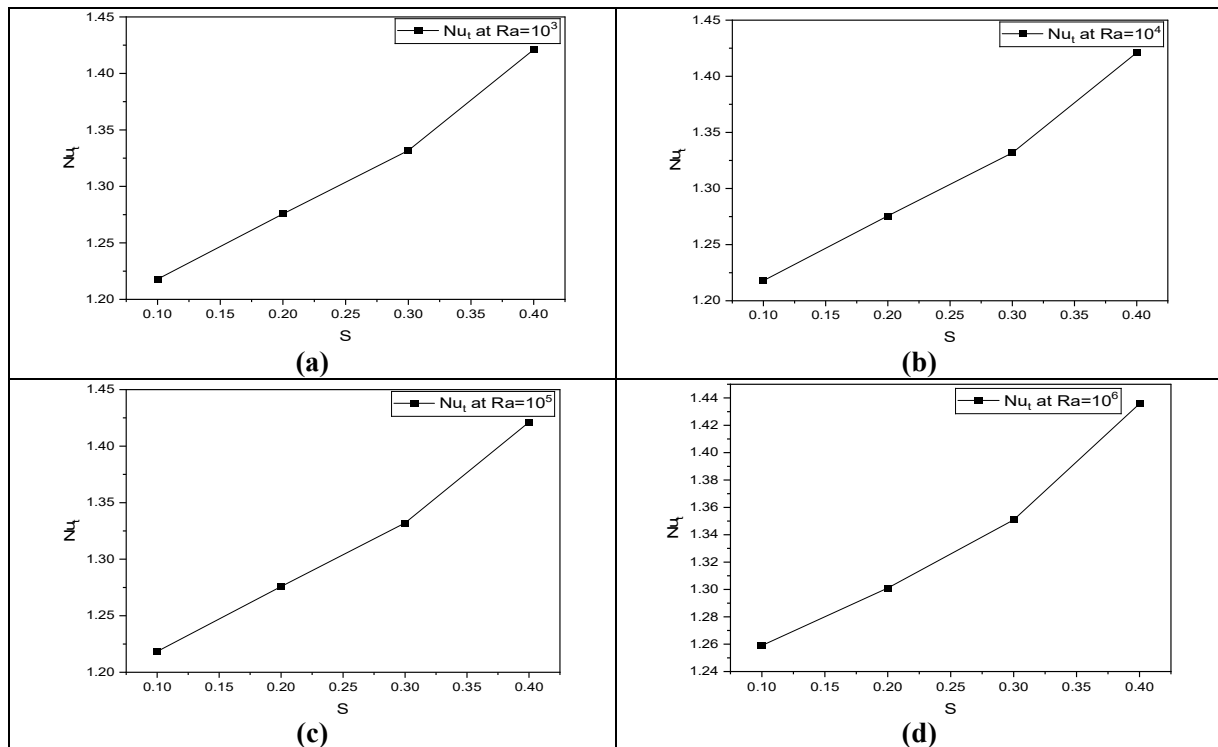
For the porous medium with $Da = 10^{-3}$ (Fig.12), the trends differ. Between $Ra = 10^3$ and $Ra = 10^4$, the Nusselt number increases by 0.02%, which illustrates that at this stage, convection is weak. However, with the increase in Ra up to 10^5 , the Nusselt number increases by 1.22% indicating that the higher permeability implies that the medium would allow for stronger convective heat transfer as permeability improves. This is even more striking at $Ra = 10^6$, where the Nusselt number increases by 22.6%, which

validates the significant role that convection plays at this increased Ra especially since permeability lets fluid flow more readily through the porous medium.

For the porous medium case at $Da = 10^{-2}$ (Fig.13), it can be found that convection is more important even at much smaller values of Ra. The rise in the Nusselt number is 0.05% when Ra varies from 10^3 to 10^4 . At an increase in Ra to 10^5 , the value of Nu rises by 5.09%, which depicts a significant enhancement in heat transfer due to convection. In the last scenario at $Ra = 10^6$, the Nusselt number increased by 26.5%, which closely resembles the results witnessed in the air medium. This high rise indicates that at higher permeability, the porous medium allows for efficient convection which is comparable to the air medium in terms of heat transfer at high Ra.

The trends are generally similar though the effect of increased spacing between the reactors is more evident at $S = 0.2$. In the air medium (Fig.10), an increase in Nusselt number by only 0.01% occurs for $Ra = 10^3$ to $Ra = 10^4$ where again it is negligible improvement in the heat transfer process. But an increase of 1.5% is observed from $Ra = 10^4$ to $Ra = 10^5$ where it depends on the improvement in convection currents which is the correct answer. The maximum change is between $Ra = 10^5$ and $Ra = 10^6$, with an increase in the Nusselt number of 28.7%, indicating that for higher Rayleigh numbers, convection is the dominant mechanism for heat transfer.

For porous medium at $Da = 10^{-4}$ (Fig.11), the percentage changes are insignificant. The Nusselt number increases only by 0.03% between $Ra = 10^3$ and $Ra = 10^4$, indicating a very minor role by convection. As Ra increases to 10^5 , the Nusselt number drops by -0.35% that even at this Ra value, porous medium continues to restrict fluid motion. For $Ra = 10^6$, Nusselt number marginally decreases by -0.1%, indicating that the low permeability continues to remain a significant problem for effective heat transfer even when Ra has increased with larger values.



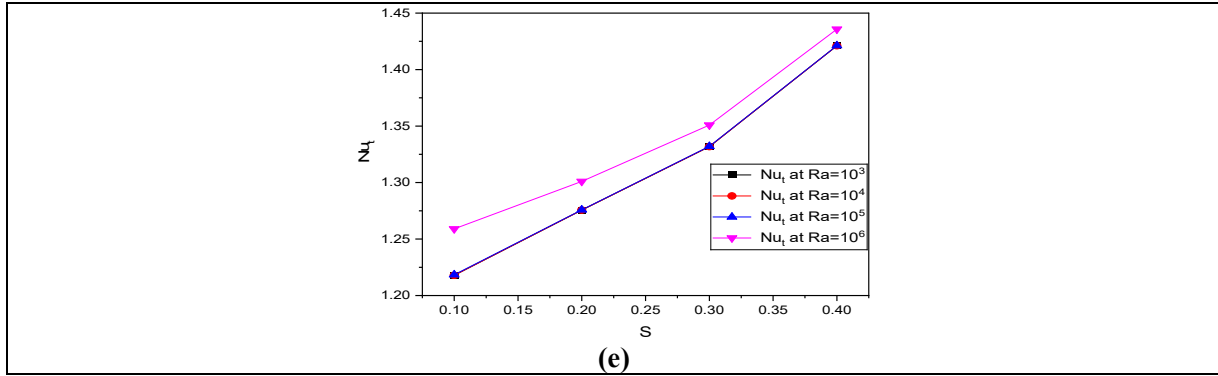
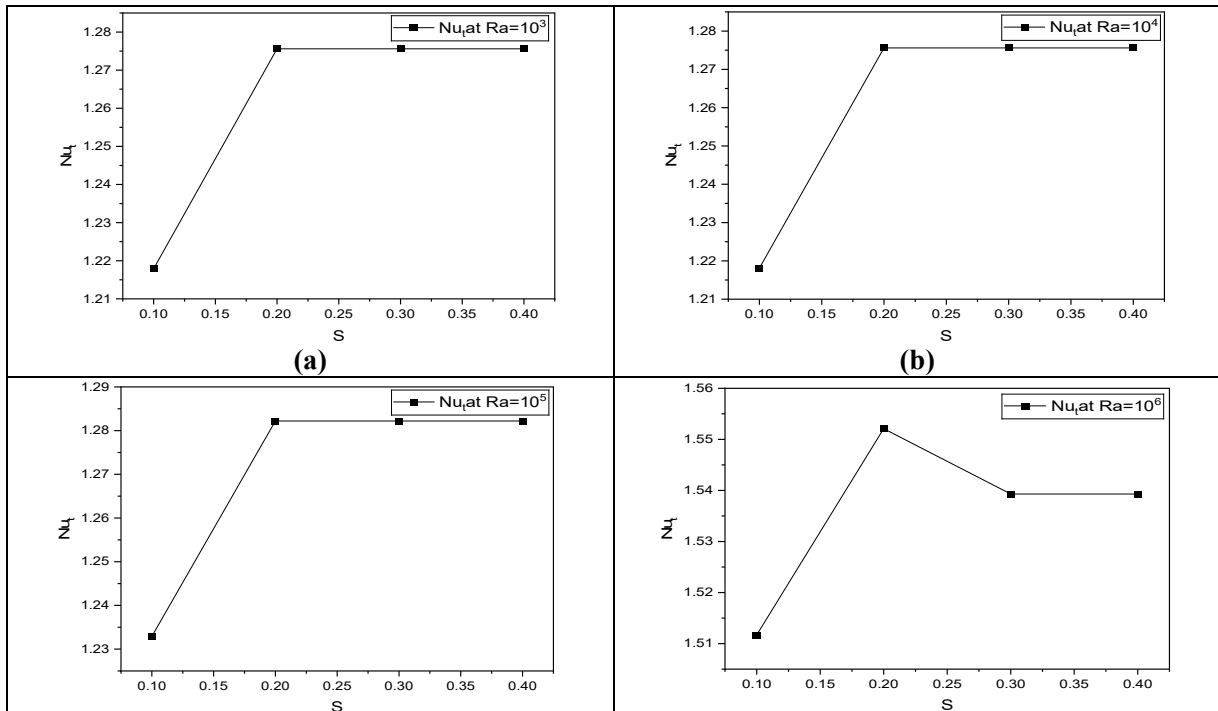


Fig.11: Spacing of Micro-Nuclear-Reactor (S) Vs Nusselt Number (Nu) at $10^3 \leq Ra \leq 10^6$ for Porous medium at $Da=10^{-4}$.

In contrast, it is seen that the porous medium with $Da = 10^{-3}$ (Fig.12) possesses greater increments of the heat transfer. It is observed that there is no appreciable variation of Nu in the range from $Ra = 10^3$ to $Ra = 10^4$, however, in the range from $Ra = 10^4$ to $Ra = 10^5$, Nusselt number increased by 0.52%. A significant augmentation of Nusselt number occurred at $Ra = 10^6$ with a percentage increase of 21.1%, which resulted because higher permeability facilitates the proper formation of convective currents and thereby improves heat transfer.

At higher Ra, the improvement is more pronounced for the porous medium with $Da = 10^{-2}$ (Fig.13). In the range of $Ra = 10^3$ to $Ra = 10^4$, the Nusselt number improves by 0.02%, showing a small improvement in heat transfer. With an increase in Ra up to 10^5 , the Nu increased by 1.91%, and at $Ra = 10^6$, the improvement is substantial at 35.05%, showing that in higher permeability conditions, it significantly enhances convective heat transfer at larger distances and higher Ra.



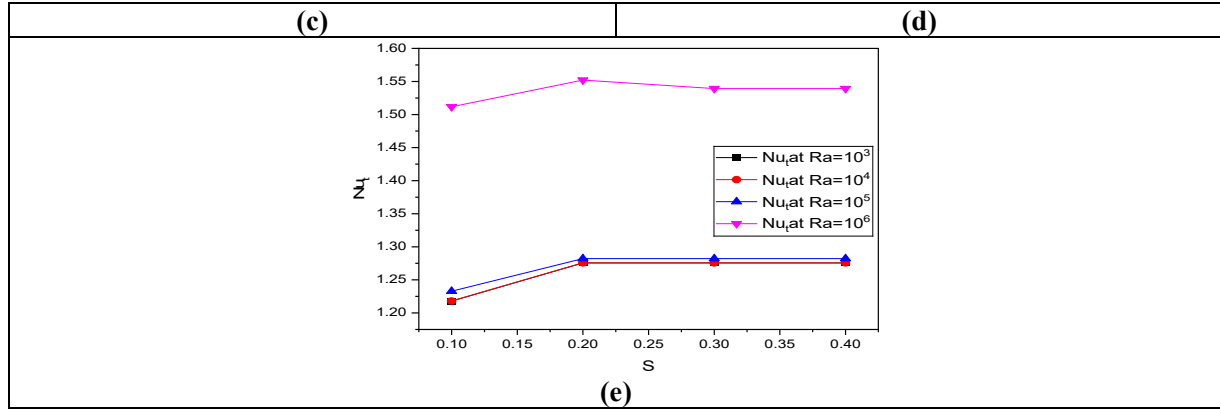


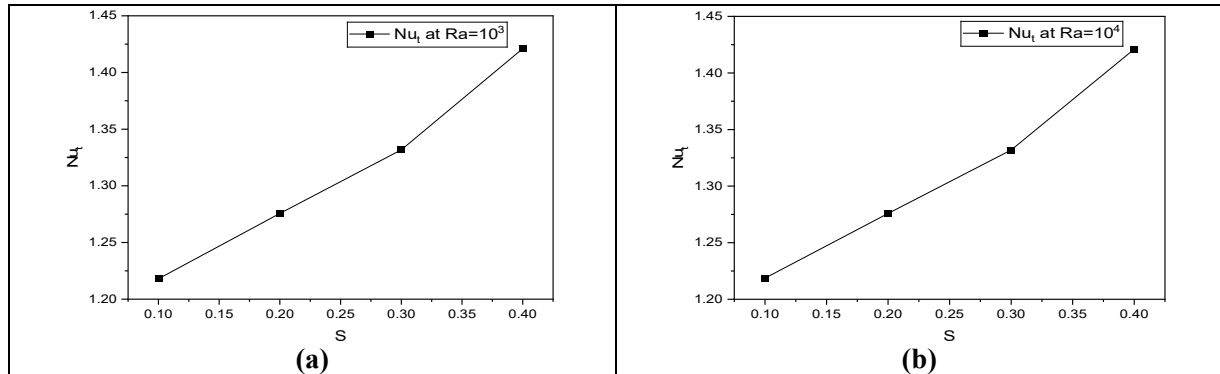
Fig.12: Spacing of Micro-Nuclear-Reactor (S) Vs Nusselt Number (Nu) at $10^3 \leq Ra \leq 10^6$ for Porous medium at $Da=10^{-3}$.

At $S = 0.3$, similar trends are noted. However, here, the impact of distance has enhanced the role of convection. In the air medium (Fig.10), the Nusselt number decreases by a minor -0.01% between $Ra = 10^3$ to $Ra = 10^4$. This reflects that the heat transfer has not undergone great changes. This trend however changes with an increase in Ra to 10^5 as the Nusselt number goes up by 1.75%, and at $Ra = 10^6$, it is large at 26.7%, which simply illustrates that at larger distances and higher Ra , convection increases.

At $Da = 10^{-4}$ in the porous medium (Fig.11), Nu rises by 0.3% from $Ra = 10^3$ to $Ra = 10^4$, meaning slight improvement of convective flow. Between $Ra = 10^4$ and $Ra = 10^5$, the Nu rises by 0.24%, and from $Ra = 10^5$ to $Ra = 10^6$, the Nu increases highly by 14.02%, meaning that at lower permeability, even then, as the reactor distance and Ra increases, the convective heat transfer will improve.

From Fig.12 Nu decreases by -3.9% from $Ra = 10^3$ and $Ra = 10^4$ for a porous medium with $Da = 10^{-3}$, which reflects the restrictions in fluid flow due to low permeability. However, as Ra approaches 10^5 , the increase in the Nu is 0.49%, and at $Ra = 10^6$, the Nu rises quite significantly by 20.1%, establishing that as Ra and permeability increase convection becomes much more effective.

For this porous medium with $Da = 10^{-2}$ (Fig.13), the Nusselt number increases a little up to 0.03% from $Ra = 10^3$ to $Ra = 10^4$, and then increases to a greater extent of 5.03% after $Ra = 10^5$ to $Ra = 10^6$. Then at $Ra = 10^6$, Nu increases significantly by 27.7% with an indication that at higher permeability and reactor distance, convection is dominating in this mode of heat transfer.



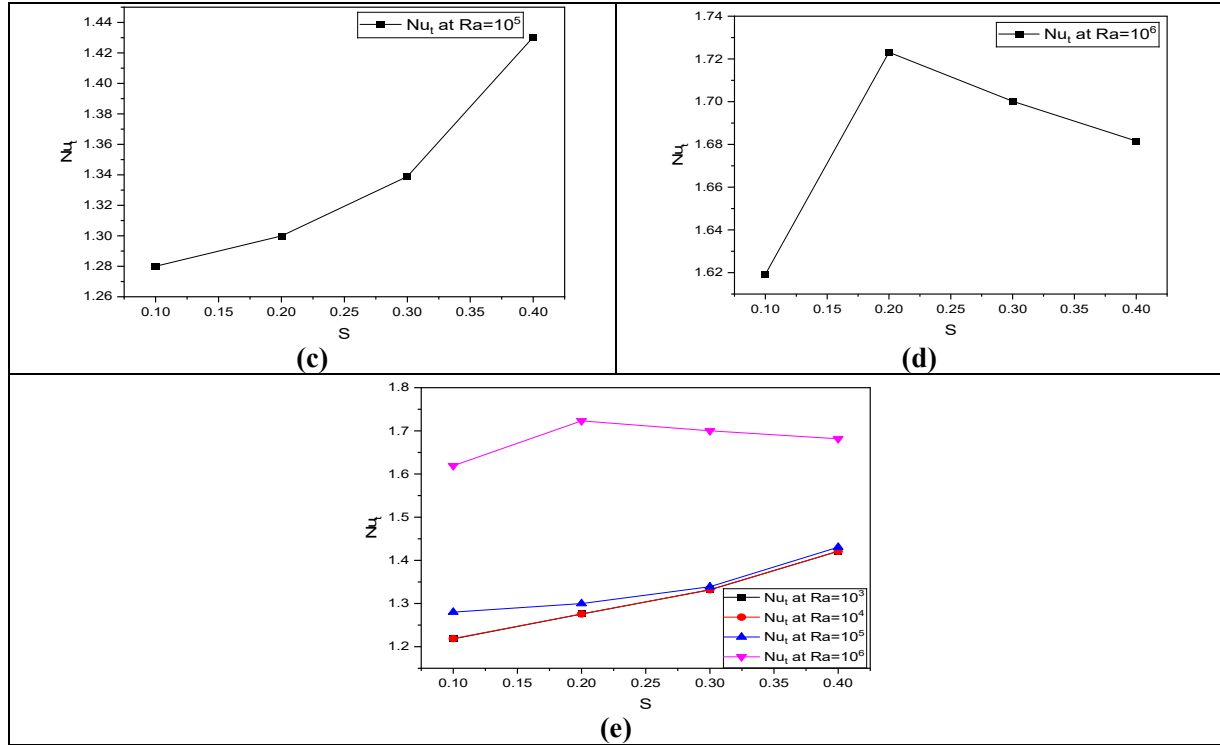


Fig.13: Spacing of Micro-Nuclear-Reactor (S) Vs Nusselt Number (Nu) at $10^3 \leq Ra \leq 10^6$ for Porous medium at $Da=10^{-2}$.

Finally, at $S=0.4$, the trends persist, but the greater distance enhances the effects of convection. While in air medium (Fig.10) as the Nusselt number was constant between $Ra=10^3$ and $Ra=10^4$ and increased by 0.71% from $Ra=10^4$ to $Ra=10^5$ followed by an increase of 18.8% from $Ra=10^5$ to $Ra=10^6$ which considerably reflects the convection forces.

For the case with $Da=10^{-4}$ (Fig.11), from $Ra=10^3$ up to $Ra=10^4$, the Nusselt number has a small increase at around 0.41%, whereas from $Ra=10^4$ to $Ra=10^5$, the increase in Nu is at 0.01%. By the time $Ra=10^6$, it gives an increase in Nu at 1.03%, which shows quite modest gains in heat transfer at lower permeability.

For the porous medium with $Da=10^{-3}$ (Fig.12), from $Ra=10^3$ to $Ra=10^4$, the Nusselt number decreases substantially by an amount of -9.87%, however, it increases by 2.46% between $Ra=10^4$ and $Ra=10^5$, and then it increases by 20.06% from $Ra=10^5$ to $Ra=10^6$. It seems that permeability in an upward direction significantly enhances the enhancement of convective heat transfer when the permeability and Ra values are increased.

In the porous medium with $Da=10^{-2}$ (Fig.13), the Nusselt number increases marginally by 0.41% from $Ra=10^3$ to $Ra=10^4$ and by 0.65% between $Ra=10^4$ and $Ra=10^5$. At $Ra=10^6$, the Nu rises perceptibly by 18.81%, thereby showing at high permeability that convection dominates the heat transfer process.

Conclusions

The paper studied the natural convection heat transfer between two embedded micro-nuclear reactors in a square enclosure filled with a porous medium. It discussed the effects of Rayleigh number, Ra, Darcy number, Da, and reactor spacing, s, on streamlines, isotherms, and Nusselt number behaviors for optimal configurations of heat transfer.

- Dependence on the Rayleigh number (Ra), by streamlines and isotherms, tenfold growth in Ra resulted approximately to tenfold growth for maximal values of stream function in both streamlines and temperature functions (T_{\max} and T_{\min}), which indicated a drift to strong convection with a stronger buoyancy force lifting motion.
- The Darcy number (Da), describes the porous medium's permeability. Fluid flow was dominated by the Darcy number, and the increase in the streamline function for $Ra = 10^6$ is almost 700 times that for $Ra = 10^3$ at $Da = 10^{-2}$.
- Temperature distribution with isotherms at low Ra values were nearly horizontal indicating the mode of heat transfer was conduction. At $Ra = 10^6$, the contours were very distorted in air and high permeability porous media, which indicated strong convective currents.
- Trends in Nusselt number in air medium at $S = 0.1$, Nusselt number increased gradually by 0.08% between $Ra = 10^3$ and $Ra = 10^4$, 5.6% between $Ra = 10^4$ and $Ra = 10^5$, and 27.27% between $Ra = 10^5$ and $Ra = 10^6$.
- At low permeability, the increase of Nu is minimal at $Da = 10^{-4}$, for this, heat transfer is permitted only in the restricted porous medium, though the convection flow is within the convection range but is also restricted between $Ra = 10^3$ to $Ra = 10^4$, this still decreases by as much as -0.32% and -3.48% at $Ra = 10^5$ and $Ra = 10^6$, respectively. This signifies that low permeability is the limiting factor for convective flow.
- The enhancement in heat transfer at $Da = 10^{-2}$ with high permeability. For Nusselt numbers, there are increments by 0.05%, 5.09%, and 26.5% as Ra varied from 10^3 to 10^6 . It means that larger permeability lets buoyancy-driven convection dominate.
- The configuration $S = 0.3$, $Ra = 10^6$, and $Da = 10^{-2}$ had the highest possibility of maximum heat transfer for fully developed, independent convection cells around each reactor as interference is minimized. In this configuration, the increase in the Nusselt number was 27.7% and, in this respect, reflects how balanced spacing, high values of Ra, and sufficiency of permeability improve heat transfer.

Reference

- [1] Aleshkova, I. A., & Sheremet, M. A. (2010). Unsteady conjugate natural convection in a square enclosure filled with a porous medium. *International Journal of Heat and Mass Transfer*, 53(23-24), 5308-5320.
- [2] Bhowmick, D., Chakravarthy, S., Randive, P. R., & Pati, S. (2020). Numerical investigation on the effect of magnetic field on natural convection heat transfer from a pair of embedded cylinders within a porous enclosure. *Journal of Thermal Analysis and Calorimetry*, 141(6), 2405-2427.

- [3] Ganapathy, R. (1997). Time-dependent free convection motion and heat transfer in an infinite porous medium induced by a heated sphere. *International journal of heat and mass transfer*, 40(7), 1551-1557.
- [4] Narasimhan, A., & Reddy, B. V. K. (2010). Natural convection inside a bidisperse porous medium enclosure.
- [5] Varol, Y., Oztop, H. F., & Yilmaz, T. (2007). Two-dimensional natural convection in a porous triangular enclosure with a square body. *International communications in heat and mass transfer*, 34(2), 238-247.
- [6] Olayemi, O. A., Khaled, A. F., Temitope, O. J., Victor, O. O., Odetunde, C. B., & Adegun, I. K. (2023). Parametric study of natural convection heat transfer from an inclined rectangular cylinder embedded in a square enclosure. *Australian Journal of Mechanical Engineering*, 21(2), 668-681.
- [7] Iyi, D., & Hasan, R. (2015). Natural convection flow and heat transfer in an enclosure containing staggered arrangement of blockages. *Procedia engineering*, 105, 176-183.
- [8] Ataei-Dadavi, I., Rounaghi, N., Chakkingal, M., Kenjeres, S., Kleijn, C. R., & Tummers, M. J. (2019). An experimental study of flow and heat transfer in a differentially side heated cavity filled with coarse porous media. *International Journal of Heat and Mass Transfer*, 143, 118591.
- [9] Nammi, G., Deka, D. K., Pati, S., & Baranyi, L. (2022). Natural convection heat transfer within a square porous enclosure with four heated cylinders. *Case Studies in Thermal Engineering*, 30, 101733.
- [10] Khanafer, K., & Vafai, K. (2020). Effect of a circular cylinder and flexible wall on natural convective heat transfer characteristics in a cavity filled with a porous medium. *Applied Thermal Engineering*, 181, 115989.
- [11] Bhowmick, D., Randive, P. R., Pati, S., Agrawal, H., Kumar, A., & Kumar, P. (2020). Natural convection heat transfer and entropy generation from a heated cylinder of different geometry in an enclosure with non-uniform temperature distribution on the walls. *Journal of Thermal Analysis and Calorimetry*, 141, 839-857.
- [12] Rasheed, S. A., & Hasan, A. J. (2022). Effect of orientation on the natural convection heat transfer from a heated triangular prism embedded in porous media. *Case Studies in Thermal Engineering*, 35, 102134.
- [13] Barman, P., & Rao, P. S. (2021). Natural convection inside a heat source embedded wavy porous cavity containing an insulated obstacle. *Proceedings of the Institution of Mechanical Engineers, Part E: Journal of Process Mechanical Engineering*, 235(5), 1694-1704.
- [14] Mercier, J. F. O., Weisman, C., Firdaouss, M., & Le Que' re', P. (2002). Heat transfer associated to natural convection flow in a partly porous cavity. *J. Heat Transfer*, 124(1), 130-143.
- [15] Nouanegue, H. F., Muftuoglu, A., & Bilgen, E. (2009). Heat transfer by natural convection, conduction and radiation in an inclined square enclosure bounded with a solid wall. *International Journal of Thermal Sciences*, 48(5), 871-880.
- [16] Shih, Y. C., Khodadadi, J. M., Weng, K. H., & Ahmed, A. (2009). Periodic fluid flow and heat transfer in a square cavity due to an insulated or isothermal rotating cylinder.
- [17] Shih, Y. C., Khodadadi, J. M., Dai, H. W., & Fan, L. (2009, January). Periodic Fluid Flow and Heat Transfer in a Square Cavity Due to an Insulated or Isothermal Rotating Rectangular Object. In *Heat Transfer Summer Conference* (Vol. 43574, pp. 853-862).

- [18] Ushachew, E. G., Sharma, M. K., & Makinde, O. D. (2021). Heat convection in micropolar nanofluid through porous medium-filled rectangular open enclosure: effect of an embedded heated object with different geometries. *Journal of Thermal Analysis and Calorimetry*, 146(4), 1865-1881.
- [19] Bhowmick, D., Chakravarthy, S., Randive, P. R., & Pati, S. (2020). Numerical investigation on the effect of magnetic field on natural convection heat transfer from a pair of embedded cylinders within a porous enclosure. *Journal of Thermal Analysis and Calorimetry*, 141(6), 2405-2427.
- [20] Basak, T., Roy, S., Paul, T., & Pop, I. (2006). Natural convection in a square cavity filled with a porous medium: effects of various thermal boundary conditions. *International Journal of Heat and Mass Transfer*, 49(7-8), 1430-1441.
- [21] Nagaraju, P. (2009). Studies on heat and mass transfer problems in saturated porous media. *university grants commission, MRP (S)-165/08-09*, 3(4).
- [22] Mishra, L., & Chhabra, R. P. (2018). Natural convection in power-law fluids in a square enclosure from two differentially heated horizontal cylinders. *Heat Transfer Engineering*, 39(10), 819-842.
- [23] Mahmood, R. A., Ibrahim, A. K., Kamilxy, A. G. M., & Saeed, R. I. (2023, July). Natural convection from a horizontal cylinder placed in a square enclosure: CFD simulations. In *AIP Conference Proceedings* (Vol. 2830, No. 1). AIP Publishing.
- [24] Chen, S., Gong, W., & Yan, Y. (2018). Conjugate natural convection heat transfer in an open-ended square cavity partially filled with porous media. *International Journal of Heat and Mass Transfer*, 124, 368-380.
- [25] Hussain, S. H., & Hussein, A. K. (2010). Numerical investigation of natural convection phenomena in a uniformly heated circular cylinder immersed in square enclosure filled with air at different vertical locations. *International Communications in Heat and Mass Transfer*, 37(8), 1115-1126.
- [26] Tong, T. W., & Subramanian, E. (1986). Natural convection in rectangular enclosures partially filled with a porous medium. *International journal of heat and fluid flow*, 7(1), 3-10.
- [27] Aly, A. M. (2020). Natural convection of a nanofluid-filled circular enclosure partially saturated with a porous medium using ISPH method. *International Journal of Numerical Methods for Heat & Fluid Flow*, 30(11), 4909-4932.
- [28] Oztop, H. F., Varol, Y., & Pop, I. (2009). Investigation of natural convection in triangular enclosure filled with porous medi saturated with water near 4° C. *Energy Conversion and Management*, 50(6), 1473-1480.
- [29] Baytaş, A. C., & Pop, I. (2001). Natural convection in a trapezoidal enclosure filled with a porous medium. *International Journal of Engineering Science*, 39(2), 125-134.
- [30] Varol, Y., Oztop, H. F., & Pop, I. (2009). Natural convection in a diagonally divided square cavity filled with a porous medium. *International Journal of Thermal Sciences*, 48(7), 1405-1415.
- [31] Baytas, A. C. (2003). Thermal non-equilibrium natural convection in a square enclosure filled with a heat-generating solid phase, non-Darcy porous medium. *International journal of energy research*, 27(10), 975-988.
- [32] Solomon, A. B., van Rooyen, J., Rencken, M., Sharifpur, M., & Meyer, J. P. (2017). Experimental study on the influence of the aspect ratio of square cavity on natural convection heat transfer with Al₂O₃/Water nanofluids. *International Communications in Heat and Mass Transfer*, 88, 254-261.
- [33] Sheikholeslami, M., Ellahi, R., Hassan, M., & Soleimani, S. (2014). A study of natural convection heat transfer in a nanofluid filled enclosure with elliptic inner cylinder. *International Journal of Numerical Methods for Heat & Fluid Flow*, 24(8), 1906-1927.

- [34] Karimdoost Yasuri, A., Izadi, M., & Hatami, H. (2019). Numerical study of natural convection in a square enclosure filled by nanofluid with a baffle in the presence of magnetic field. *Iranian Journal of Chemistry and Chemical Engineering*, 38(5), 209²20.
- [35] Ho, C. J., Liu, W. K., Chang, Y. S., & Lin, C. C. (2010). Natural convection heat transfer of alumina-water nanofluid in vertical square enclosures: An experimental study. *International Journal of Thermal Sciences*, 49(8), 1345-1353.
- [36] Garbadeen, I. D., Sharifpur, M., Slabber, J. M., & Meyer, J. P. (2017). Experimental study on natural convection of MWCNT-water nanofluids in a square enclosure. *International Communications in Heat and Mass Transfer*, 88, 1-8.
- [37] Boulahia, Z., Wakif, A., & Sehaqui, R. (2016). Natural convection heat transfer of the nanofluids in a square enclosure with an inside cold obstacle. *International journal of innovation and scientific research*, 21(2), 367-375.
- [38] Mohebbi, R., Izadi, M., & Chamkha, A. J. (2017). Heat source location and natural convection in a C-shaped enclosure saturated by a nanofluid. *Physics of Fluids*, 29(12).
- [39] Cho, H. W., Ha, M. Y., & Park, Y. G. (2019). Natural convection in a square enclosure with two hot inner cylinders, Part II: The effect of two elliptical cylinders with various aspect ratios in a vertical array. *International Journal of Heat and Mass Transfer*, 135, 962-973.
- [40] Charreh, D., Islam, S. U., Talib, S., Saleem, M., Abbas, M. A., & Ahmad, S. (2024). Numerical investigation of entropy generation and Magnetohydrnamic natural convection in a porous square cavity with four embedded cylinders. *Heliyon*, 10(13).
- [41] Karimi, Fariborz, Hong Tao Xu, Zhiyun Wang, Mo Yang, and Yuwen Zhang. "Numerical simulation of unsteady natural convection from heated horizontal circular cylinders in a square enclosure." *Numerical Heat Transfer, Part A: Applications* 65, no. 8 (2014): 715-731.